Examining the status of forest fire emission in 2020 and its connection to COVID-19 incidents in West Coast regions of the United States

Srikanta Sannigrahi [a,*], Francesco Pilla [a], Arabinda Maiti [b], Somnath Bar [c], Sandeep Bhatt [d], Ankit kaparwan [e], Qi Zhang [f], Saskia Keesstra [g,h], Artemi Cerda [i]

[a] School of Architecture, Planning and Environmental Policy, University College Dublin Richview, Clonskeagh, Dublin, D14 E099, Ireland
[b] Department of Geography, Vidyasagar University, Midnapore, West Bengal, India
[c] Department of Geoinformatics, Central University of Jharkhand, Ranchi, India
[d] Department of Earth Sciences, Indian Institute of Technology Roorkee, India
[e] Department of Statistics, Hemvati Nandan Bahuguna Garhwal University, Srinagar, India
[f] Department of Geography, University of North Carolina at Chapel Hill, Chapel Hill, NC 27599, USA
[g] Team Soil, Water and Land Use, Wageningen Environmental Research, Wageningen University & Research, Wageningen, Netherlands
[h] Civil, Surveying and Environmental Engineering and Centre for Water Security and Environmental Sustainability, The University of Newcastle, Callaghan, 2308, Australia
[i] Soil Erosion and Degradation Research Group, Department of Geography, Valencia University, Blasco Ibàñez, 28, 46010, Valencia, Spain

ARTICLE INFO

ABSTRACT

Forest fires impact on soil, water, and biota resources. The current forest fires in the West Coast of the United States (US) profoundly impacted the atmosphere and air quality across the ecosystems and have caused severe environmental and public health burdens. Forest fire led emissions could significantly exacerbate the air pollution level and, therefore, would play a critical role if the same occurs together with any epidemic and pandemic health crisis. Limited research is done so far to examine its impact in connection to the current pandemic. As of October 21, nearly 8.2 million acres of forest area were burned, with more than 25 casualties reported so far. In-situ air pollution data were utilized to examine the effects of the 2020 forest fire on atmosphere and coronavirus (COVID-19) casualties. The spatial-temporal concentrations of particulate matter ($PM_{2.5}$ and PM_{10}) and Nitrogen Dioxide (NO_2) were collected from August 1 to October 30 for 2020 (the fire year) and 2019 (the reference year). Both spatial (Multiscale Geographically Weighted Regression) and non-spatial (Negative Binomial Regression) analyses were performed to assess the adverse effects of fire emission on human health. The in-situ data-led measurements showed that the maximum increases in $PM_{2.5}$, PM_{10}, and NO_2 concentrations ($\mu g/m^3$) were clustered in the West Coastal fire-prone states during August 1 – October 30, 2020. The average concentration ($\mu g/m^3$) of particulate matter ($PM_{2.5}$ and PM_{10}) and NO_2 was increased in all the fire states severely affected by forest fires. The average $PM_{2.5}$ concentrations ($\mu g/m^3$) over the period were recorded as 7.9, 6.3, 5.5, and 5.2 for California, Colorado, Oregon, and Washington in 2019, increasing up to 24.9, 13.4, 25.0, and 17.0 in 2020. Both spatial and non-spatial regression models exhibited a statistically significant association between fire emission and COVID-19 incidents. Such association has been demonstrated robust and stable by a total of 30 models developed for analyzing the spatial non-stationary and local association. More in-depth research is needed to better understand the complex relationship between forest fire emission and human health.

1. Introduction

Forest fire becomes a global environmental threat across ecosystems, causing severe public health burdens via the upsurges of smokes and particulate matter concentration into the lower atmosphere (Henderson et al., 2011; Bowman and Johnston, 2005; Fowler, 2003; Goldammer et al., 2008; Iriti et al., 2020). Amongst the causal factors, climate change and the associated factors (rising temperature, long dry spell,
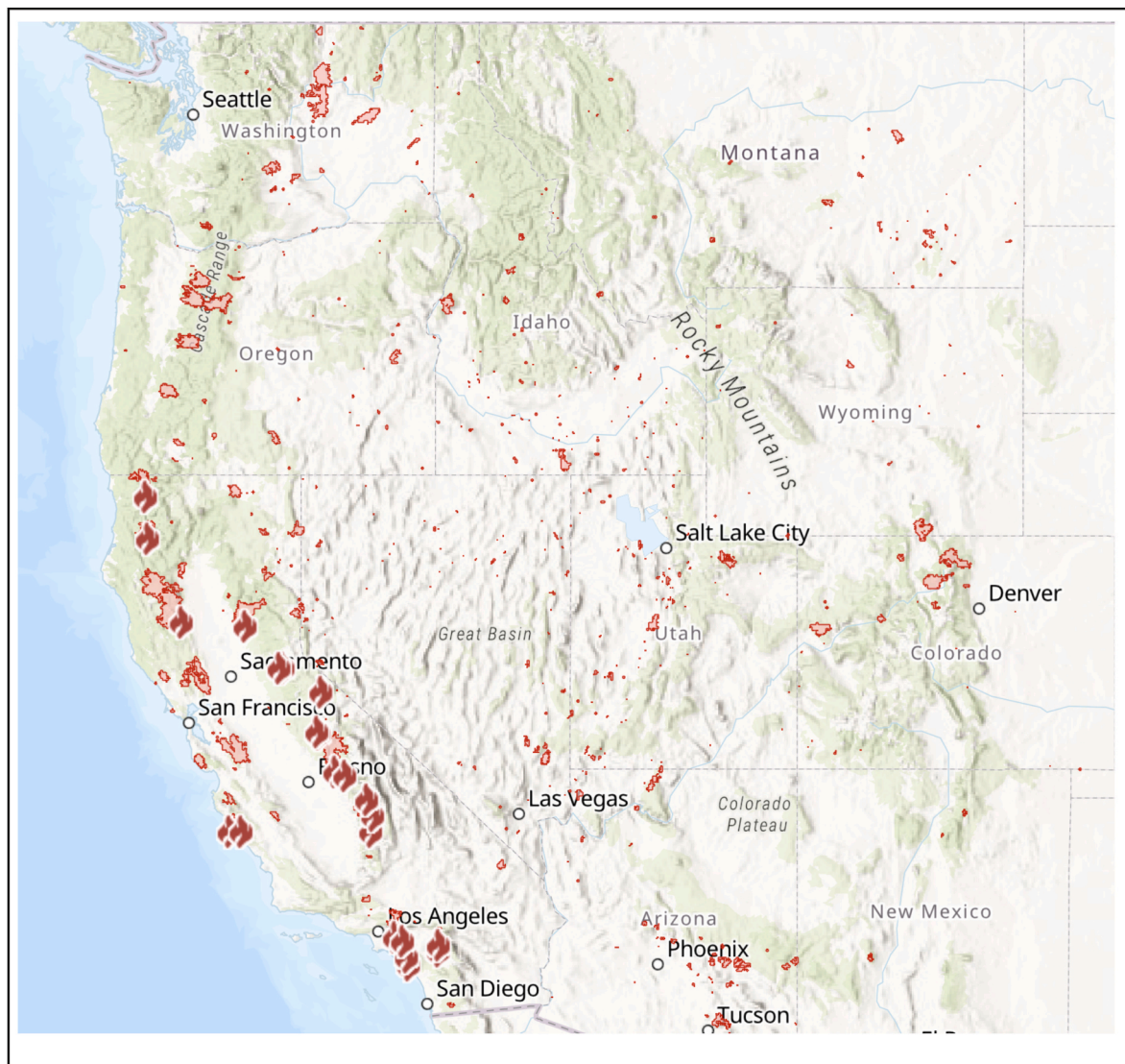
Fig. 1. Major fire events occurred in the West Coast States of the USA, mainly in California, Oregon, Washington, and Colorado in 2020.

lack of soil moisture, the abundance of flammable materials, etc.) have augmented the severity and intensity of fire incidents, extended the length of forest fire season, and eventually increased the exposure to hazardous air pollutants in the areas prone to forest fire (Aponte et al., 2016; Flannigan et al., 2000; Mateus and Fernandes, 2014; Meira Castro et al., 2020; Michel Arbez et al., 2001). Forest fire has been significantly associated with the increases in gaseous emissions, i.e. Carbon (Aragão et al., 2018; Lazaridis et al., 2008; Lü et al., 2006), Smoke (Fromm and Servranckx, 2003; Johnston et al., 2014; Mott et al., 2002), black Carbon (Badarinath et al., 2007; Jeong et al., 2004), aerosol (Pio et al., 2008; Randerson et al., 2006), fine (Ikemori et al., 2015; McLean et al., 2015; Sapkota et al., 2005) and coarse particulate matter (Henderson et al., 2008; Juneng et al., 2009), Nitrogen oxides (McEachern et al., 2000; Spichtinger et al., 2001), and other pollutants (NO, O_3, VOC) (Cheng et al., 1998). In Greece, forest fire emission was found to be the most significant contributor to the air pollution problem during the fire occurrence period (Cheng et al., 1998). Through long- and short-range atmospheric transport, forest fire emissions have had impacts on a large region from the source (Lazaridis et al., 2008). The effects of forest fire emission on air pollution can be easily detected in rural areas where anthropogenic emission is limited (Cheng et al., 1998). In the rural region of Edmonton (Canada), the hourly NO_x, O_3 concentration was recorded 50–150% higher than the seasonal median values, which can

be attributed to the forest fire and resulted in emission (Cheng et al., 1998). However, the forest fire emitted pollutants can travel thousands of kilometres with the help of upper atmospheric circulation and exacerbate the problem of local air pollution in the heavily polluted regions (Sapkota et al., 2005). The deterioration of air quality in Baltimore city (located nearly 1100 km away from the fire source region) due to 2002 Canadian forest fires has once again proven the fact that forest fire emission not only poses threats to the nearby communities, but the same can have substantial public health impact to the regions located far away from the fire-affected areas (Sapkota et al., 2005).

Several earlier research has utilized many available resources, i.e. satellite estimates (Konovalov et al., 2011; Wu et al., 2006), in-situ measurement (Konovalov et al., 2011), low-cost sensor measurements (Delp and Singer, 2020; Sayahi et al., 2019), air pollution models (Watson et al., 2019) to examine the detrimental impact of forest fires on air quality across the ecosystems. Wu et al. (2006) noted that the concentration of PM_{10} was increased up to 160 µg/m³ due to the 2003 southern California forest fires and resulted in the emission of particulate matter. Studying on 2003 European forest fires, Hodzic et al. (2007) documented a drastic increase (20–200%) of air pollutants, especially PM_{10} due to the emission of gaseous compounds during the fire period. Forest fires were also found to be highly associated with the increases of fine particulate matter ($<_{2.5}$µm) (Jaffe et al., 2008; Matz et al., 2020;
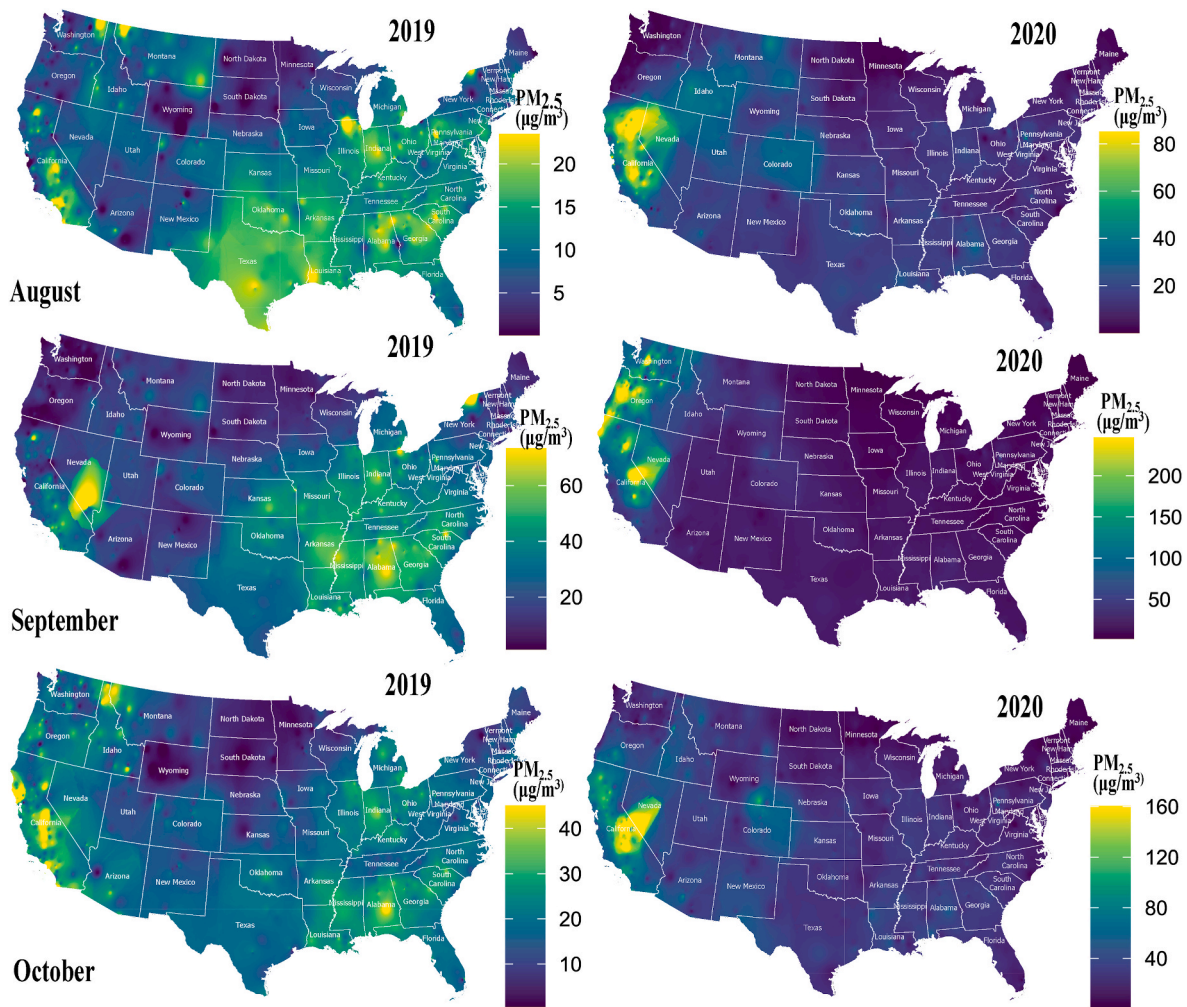
Fig. 2. Spatial distribution of PM$_{2.5}$ concentration in August, September, and October in 2019 and 2020.

Sullivan et al., 2008). Although there has been strong and clear evidence that forest fires have a strong negative impact on air quality, still, there are several other confounding factors, such as the description of fire emissions, atmospheric dispersion of smoke, and the chemical transformations of smoke, needing to be comprehensively evaluated to understand the association between forest fire and air quality in a better way (Martins et al., 2012).

Several studies have reported the association between short- or long-term exposure to air pollution and incidents of severe acute respiratory syndrome coronavirus 2–2019 (SARS-CoV-2 – COVID-19) in many regions across the world (Ogen, 2020; Sciomer et al., 2020; Shen et al., 2020; Wang et al., 2020; Zhu et al., 2020). Amongst the key air pollutants, the concentration of particulate matter (PM$_{2.5}$ and PM$_{10}$) and its association with COVID-19 casualties has been the central focus in these studies. Zhu et al. (2020) has performed Generalized Additive Model (GAM) after considering COVID-19 incidences of 120 cities in China and found that a 10 μg/m^3 increases PM$_{2.5}$ and PM$_{10}$ was associated with a 2.24% and 1.76% increase in daily COVID-19 confirmed cases. Zhu et al. found that per 10 μg/m^3 increase of NO$_2$ was associated with a 6.94% increase in daily COVID-19 confirmed cases. Yao et al. (2020) analyzed the linkages between air pollution and COVID incidences in 49 cities in China using a multiple linear regression model and found that per 10 μg/m^3 increase in PM$_{2.5}$ and PM$_{10}$ was associated with a 0.24% (0.01%–0.48%) and 0.26% (0.00%–0.51%) increase in the daily COVID-19 fatality rate (Wu et al., 2020). observation considered 3000 counties of the US and performed a zero-inflated negative binomial model to examine the linkages between the concentration of PM$_{2.5}$ and COVID death rate

during the January to April 4 (2020) period. They have reported that a 1 μg/m^3 long-term exposure increase in PM$_{2.5}$ was associated with a 15% increase in COVID-19 death rate. In England (Travaglio et al., 2021), study had found a strong association between PM$_{2.5}$ concentration and COVID incidents (an increase of 1 μg/m^3 in the long-term average of PM$_{2.5}$ was associated with a 12% increase in COVID-19 cases). Although most of these referred studies have found a strong association between air pollution level and COVID casualties, more data-driven in-depth analysis in needed to examine the role of other confounding factors in COVID casualties across the word.

The unprecedented and record-breaking forest fire events in 2020 in the West Coast states (California, Oregon, Washington, Colorado) in the US can cause severe health burdens, especially at the time of the COVID-19 pandemic. As of October 21, 2020, nearly 8.2 million acres (33,000 km^2) of forest area were burnt, and 46 casualties have been reported so far (https://www.fire.ca.gov/). The economic cost attributed to these events can be as much as $2.707 Billion in 2020 unit price. The air quality during the fire periods has become extremely poor and reached very unhealthy to hazardous level in many fire-affected regions. Although the air quality has improved in some parts of the area due to lockdown measures, it still remains hazardous in the areas poorly affected by the forest fire. Since it has been proven that forest fire contributes substantially to adding gaseous and particulate matter concentration into the lower and upper atmosphere, the coexistence of two extreme events, i.e. the 2020 forest fire, which has declared as the most intense forest fire in the US since 2003, and COVID-19 pandemic, which is also announced as one of the worst pandemics in the history of human
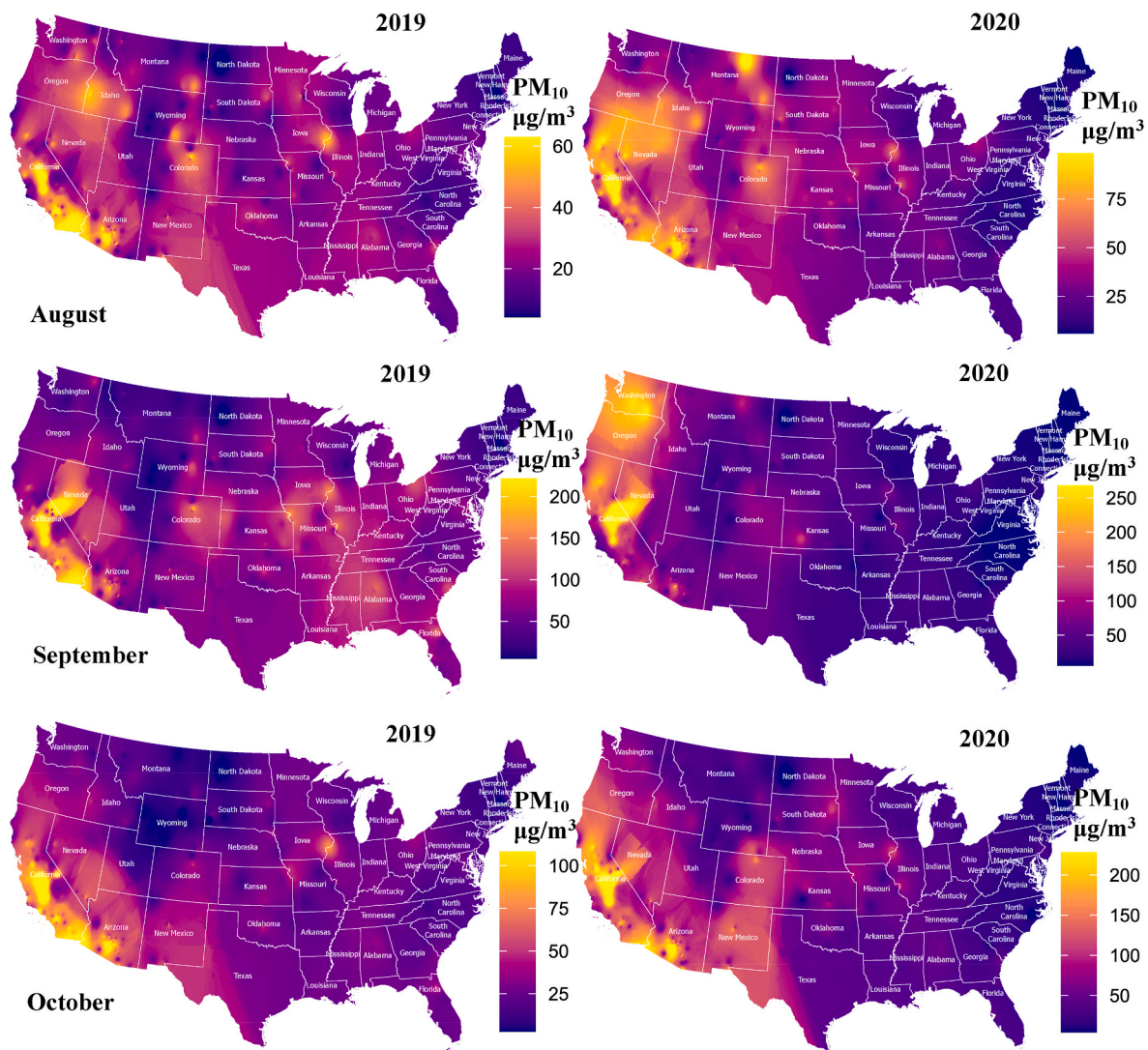
Fig. 3. Spatial distribution of PM_{10} concentration in August, September, and October in 2019 and 2020.

civilization, has not been discussed thoroughly. Therefore, the synergistic association between these two rare events (West Coast forest fire and COVID casualties) and their combined effects on human health should be examined so that the same would allow us to understand how climate change led extremities can exacerbate the crisis of public health. The objectives of this are: (1) examine the air quality levels during the fire period (August 01 to October 30) in fire year (2020) and reference year (2019), (2) measures the changes in air quality due to forest fire; (3) analzying the association between fire emission and COVID incidences using spatial regression models.

2. Materials and methods

2.1. Data source and processing

The Western states of the US, mainly California, Oregon, Washington, Idaho, Colorado, have witnessed the record-breaking (surpassed the last 18 years fire severity records in terms of forest area burnt and damages of property and structures) forest fires that started early in August 2020. As of Mid-October 2020, 8.2 million acres (33,000 square kilometres) were burned, and at least 46 casualties have been reported so far (National Interagency Fire Center). Many factors, including climate change, led to an extremely higher temperature, lack of surface moisture due to below-normal precipitation in the preceding seasons,

extended dry spell and associated heat waves, higher wind speed, abundant fuel load, etc. have exacerbated the severity and length of the forest fires in these regions (Balch et al., 2017; Collins et al., 2019; Kane et al., 2017).

In-situ air pollution measurements were retrieved from OpenAQ.[1] OpenAQ is a non-profit organization aiming to retrieve, harmonize, share open-air quality information to citizens and organizations, and provide an up-to-date status of clean air, which would eventually help prevent air pollution led health burdens across the world. The OpenAQ platform retrieved the latest and up-to-date air quality data from multiple sources such as government/institution air quality monitoring stations and low-cost open-air quality sensors. All the data were collected from August 1 to October 30 period for comparative assessment and subsequent interpretation.

Daily COVID-19 cases and death data were collected from USA-Facts.[2] The USAFacts collects COVID counts data from the Center for Disease Control and Prevention (CDC), State and local-level public health agencies. The county-level data for each States collects and verified with the local and State agencies. The daily cumulative sum of deaths and cases reports for each administrative units were recorded

---

[1] https://openaq.org/.

[2] https://usafacts.org/visualizations/coronavirus-covid-19-spread-map/.
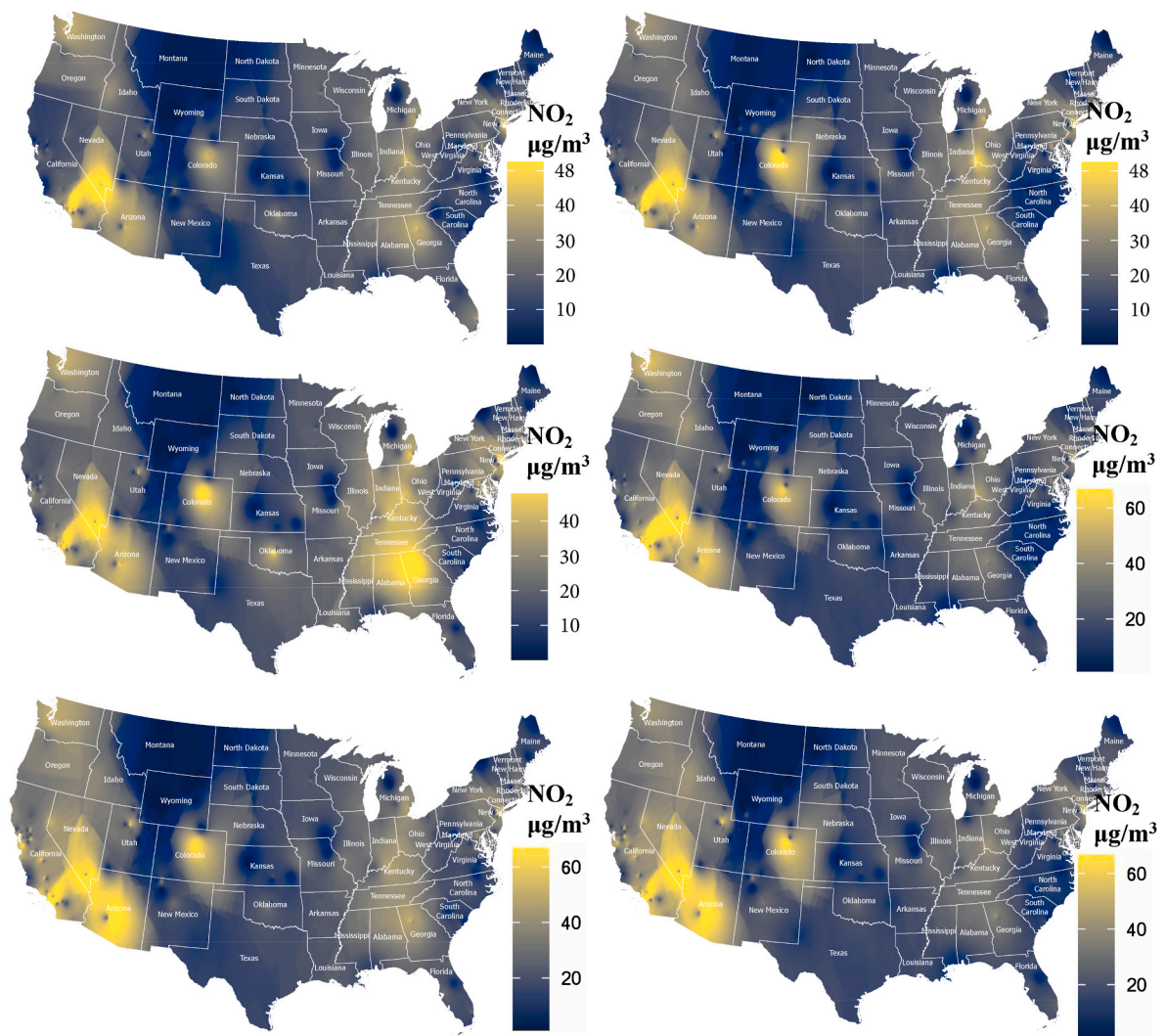
Fig. 4. Spatial distribution of NO2 concentration in August, September, and October in 2019 and 2020.
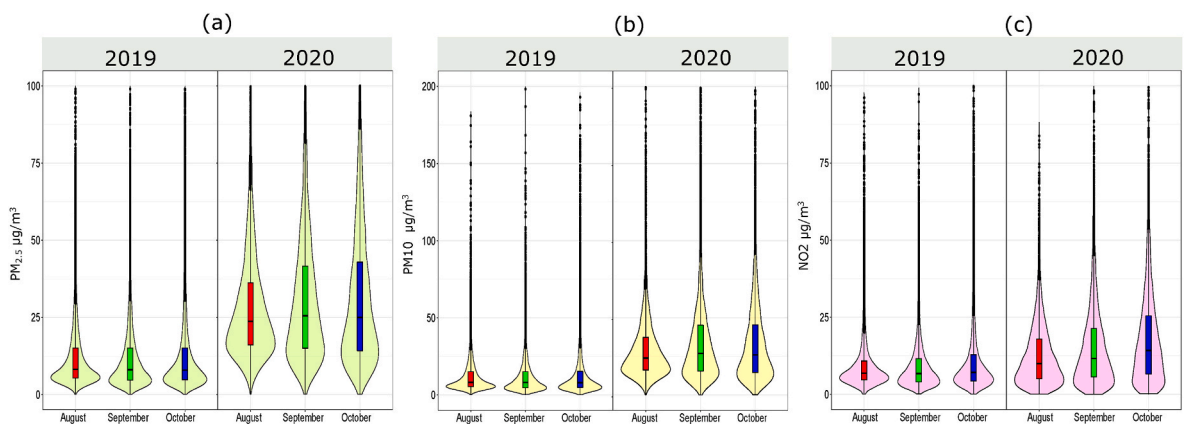
Fig. 5. Average concentration of different air pollutants (PM$_{2.5}$, PM$_{10}$, NO$_2$) in August, September, and October in 2019 and 2020.

through manual entry or web scraping (USAFacts, 2020). For California and Texas, USAFacts gather COVID data from each county's public health website. Currently, the presumptive positive cases considered as confirmed cases, which is in line with CDC's COVID reporting. Daily and cumulative sum counts of cases and deaths were analyzed to find its association with forest fire emissions. More details about the COVID

data collection process, quality assurance, data collection assumptions, flag detection and reporting, etc., can be found on the USAFacts website.

Fig. 6. Average concentration of (a) PM$_{2.5}$, (b) PM$_{10}$, (c) NO$_2$ in different States in USA in 2019 and 2020; and concentration of (d) PM$_{2.5}$, (e) PM$_{10}$, and (f) NO$_2$ in fire prone States in the USA in 2019 and 2020.
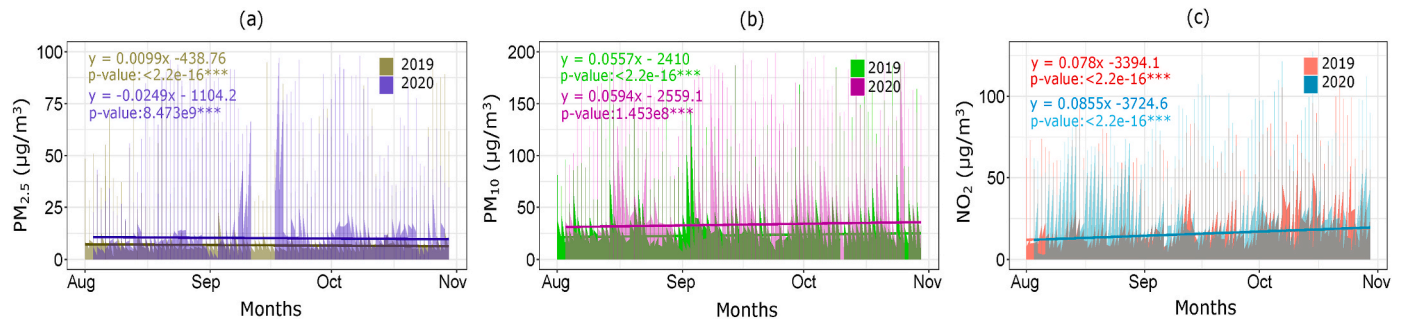
Fig. 7. Daily variation in PM$_{2.5}$, PM$_{10}$, and NO$_2$ concentration during August 01 to October 30 period in 2019 and 2020.

2.2. Regression analysis

2.2.1. Non-spatial regression model

Two regression models, i.e. Ordinary Least Square (OLS) and Negative Binomial Regression was performed to examine the association between forest fire emission and COVID incidences at the county scale. For regression analysis, only fire States were considered. OLS measures the interaction and association between the sets of dependent and independent factors (Maiti et al., 2021; Mollalo et al., 2020; Oshan et al.,

2019; Sannigrahi et al., 2020a, 2020b). Additionally, OLS fits a line based on the characteristics of the dependent and independent observations in the bivariate data framework to minimize the squared distance of each data points from the fitted line (Kilmer and Rodríguez, 2017; Sokal et al., 1995). The OLS can be formed as follows

$$y_i = a + \beta x_i + \varepsilon_i \tag{1}$$

where a is the intercept, β vector of regression coefficients, xi is the vector of selected air pollutants at county i, ε_i is the error term.

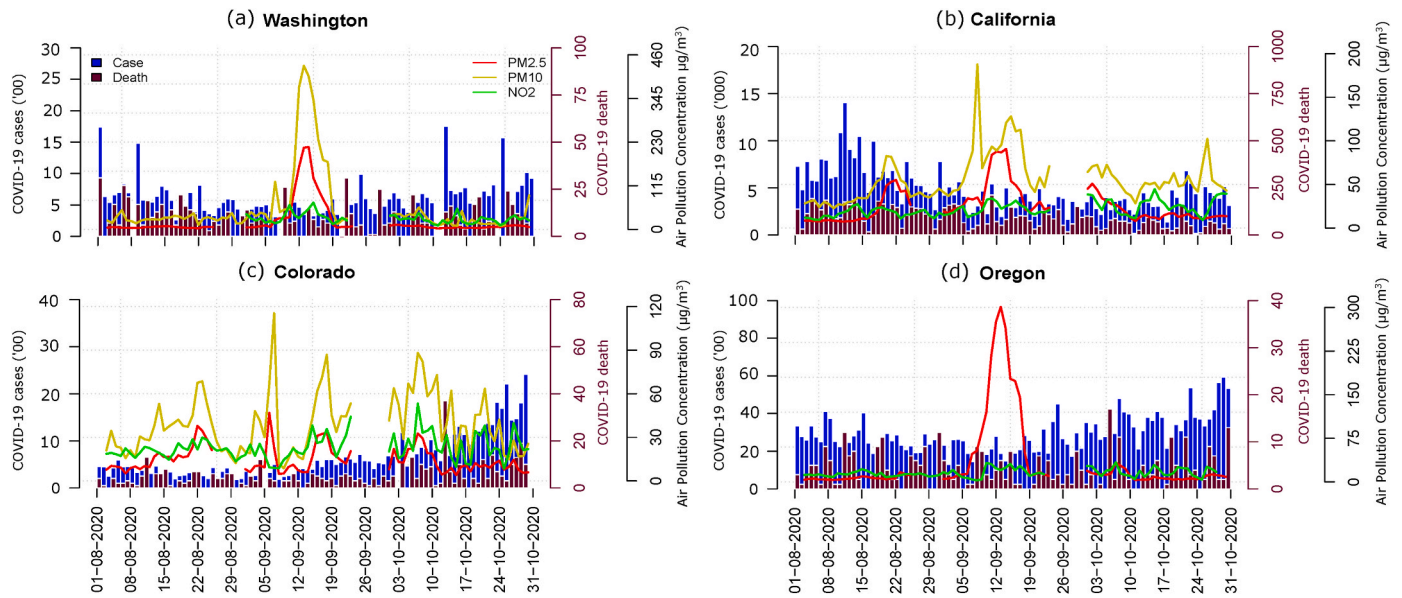**Fig. 8.** Daily changes in air pollutants (PM$_{2.5}$, PM$_{10}$, NO$_2$) and COVID-19 new cases and deaths in the four fire States during August 1 to October 30 period.

Table 1
Non-parametric test to evaluate mean differences in PM$_{2.5}$, PM$_{10}$, and NO$_2$ concentration between fire (2020) and reference (2019) year.

Month	Model	V	Expected value	Variance (V)	P-value (Two-tailed)	α
August	Model 1	212	612.5	10106.25	<0.0001	0.05
	Model 2	117	351.5	4393.75	0.000	0.05
	Model 3	540	370.5	4754.75	0.014	0.05
September	Model 4	416	612.5	10106.25	0.051	0.05
	Model 5	168	351.5	4393.75	0.006	0.05
	Model 6	621	370.5	4754.75	0.000	0.05
October	Model 7	94	612.5	10106.25	<0.0001	0.05
	Model 8	87	351.5	4393.75	<0.0001	0.05
	Model 9	438	370.5	4754.75	0.331	0.05

In addition to the standard OLS estimates, the negative binomial (NB) regression method was also applied for analyzing the association between forest fire emission and associated COVID case/death counts during the fire period (Copat et al., 2020; Wu et al., 2020). The NB regression model was used in the present research to minimize over-dispersion in statistical estimates. Among the several link function, the log has been used as a link function to carry out the NB regression analysis. The NB regression with Poisson parameter can be expressed as follows:

$$\iota_n(\lambda_i) = \beta_0 + \sum\nolimits_{k=1}^{p} \beta_k X_{ik} + \theta_i \tag{2}$$

where the Poisson parameter (λ_i) represents the expected estimates of observation i, β_0, β_k are the model input parameters, X_{ik} is the kth number of the independent variable for observation i, θ_i is the gamma-distributed error (e) term with mean and variance considered as 1 and α (Chang, 2005; Wang et al., 2021).

2.2.2. Spatial regression model

In the present study, a modified version of Geographically weighted regression (GWR) – MGWR, developed by Oshan et al. (2019), has been used for exploring the spatially varying association between the fire emission and COVID counts at county scale in the contiguous US. The GWR is a local spatial regression approach conceptualized upon the assumption of spatial heterogeneity and spatial non-stationarity among the parameters in a feature space. Unlike global regression, which assumes a spatial homogeneity and constant relationship among the features, the GWR often increases the model fit by reducing residuals of spatial autocorrelation in parameter estimates. GWR is also sensitive to bandwidth and kernel selection and parametrization, which seeks special attention while designing the spatial models to explain any spatial varying relationship between parameters.

Recently, an extension to the existing GWR frameworks known as multiscale GWR (MGWR) allows exploring the locally varying association between the parameters at a unique spatial scale which eventually helps to understand the multiscale analysis of spatial heterogeneity and spatial non-stationarity. MGWR that eliminates the assumption and limitation of the existing GWR that all spatial association vary uniformly at all spatial scale could reduce the model overfitting, spatial autocorrelation and uncertainty that mainly originates from the scale-dependent approximation of parameters. In the present study, the MGWR model incorporated into the spatial analysis framework to explore the spatial association between forest fire emission and COVID counts at the lowest spatial in the contiguous US. The mgwr python package, which has many dependencies, such as NumPy, SciPy, pandas, matplotlib, libpysal, and spglm, was used to run the MGWR model. A standard GWR model can be expressed as:

$$y_i = \beta_{i0} + \sum_{k=1}^{\rho} \beta_{ik} x_{ik} + \varepsilon_i \tag{3}$$

where y_i is the dependent variable (COVID case/death in this study) for location i, β_{i0} is the intercept coefficient of location i, β_{ik} is the local regression coefficient of k th explanatory variable at location i, x_{ik} is the kth independent variable at location i, ε_i is the random error term at location i.

In the MGWR model, the scale or bandwidth dependent spatial assumption in the GWR model has been respecified by incorporating scale variant association between the parameters in feature space as follows:
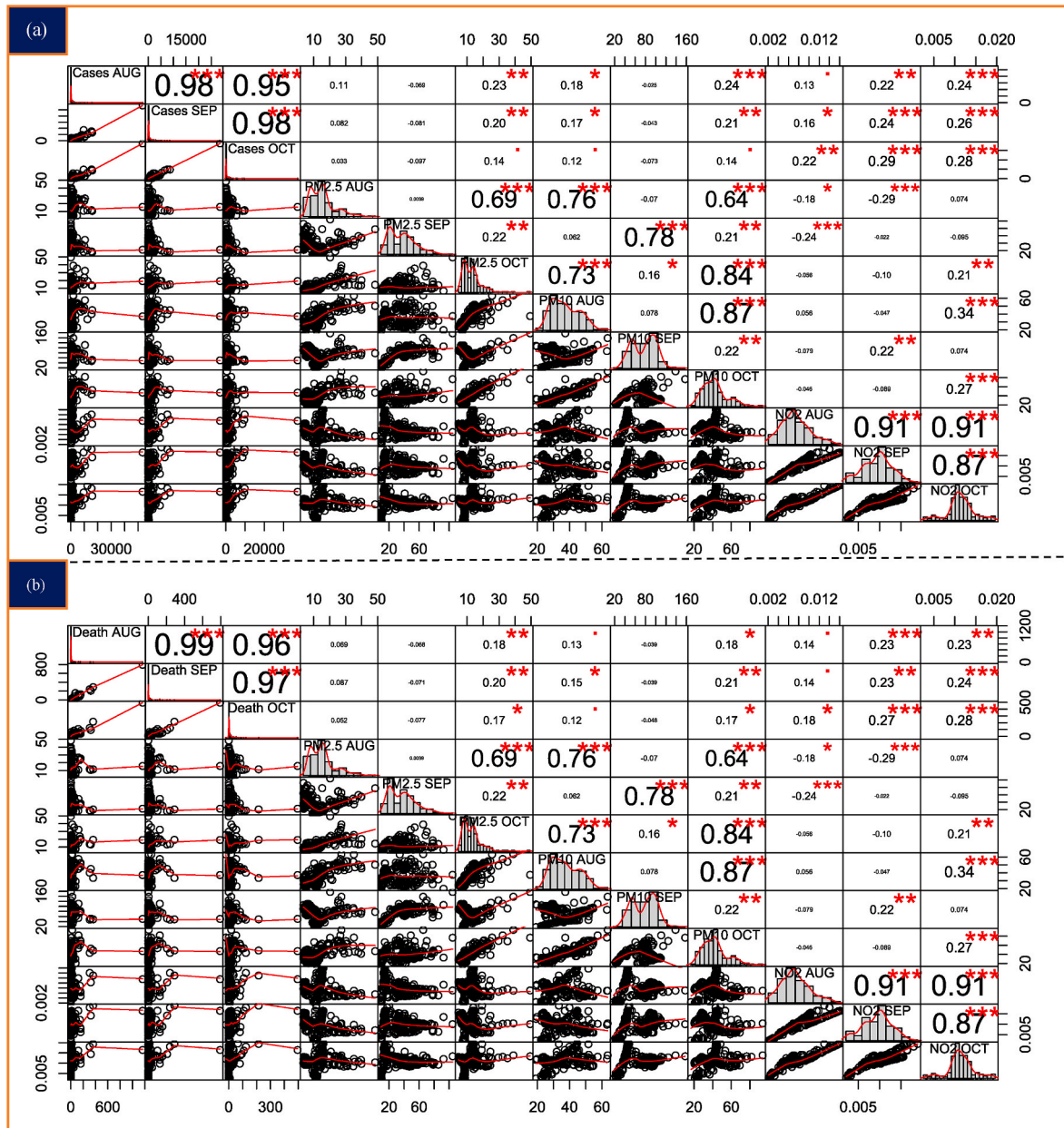
Fig. 9. Correlation matrix shows the association between monthly concentration values of PM$_{2.5}$, PM$_{10}$, and NO$_2$ and monthly average COVID incidents.
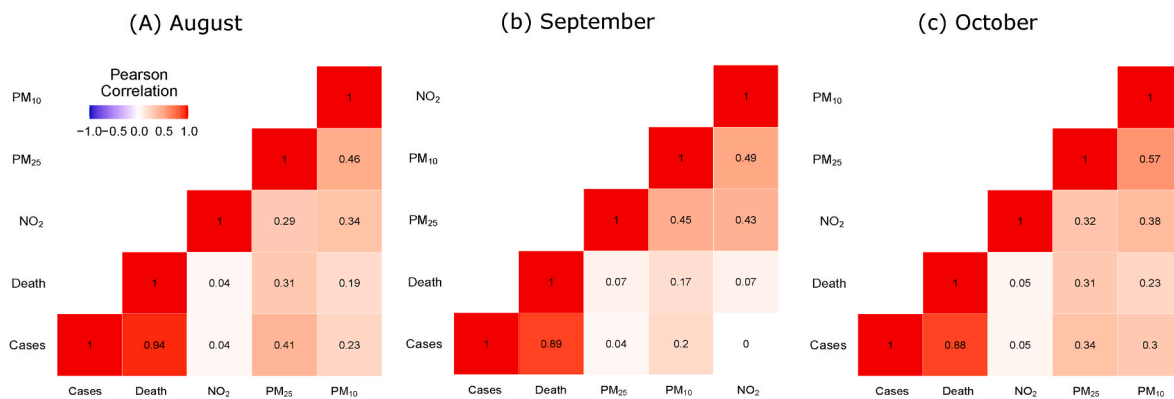

Fig. 10. Correlation matrix shows the association between the air pollution estimates and COVID-19 casualties during the entire study period (August 1 to October 30).

Table 2

Spearman correlation matrix showing the linear association between air pollution and COVID incidents in different months. Bold values are statistically significant at different probability levels.

Month	N	Model	Max		Mean		Sum	
			r	P value	r	P value	r	P value
August	196	PM$_{2.5}$ & Cases	**0.21**	**0.00**	**0.16**	**0.02**	0.14	0.06
		PM$_{10}$ & Cases	**0.32**	**0.00**	**0.27**	**0.00**	**0.17**	**0.02**
		NO$_2$ & Cases	0.09	0.22	−0.03	0.68	0.09	0.22
September		PM$_{2.5}$ & Cases	**0.25**	**0.00**	**0.22**	**0.00**	**0.18**	**0.01**
		PM$_{10}$ & Cases	**0.31**	**0.00**	**0.26**	**0.00**	**0.18**	**0.01**
		NO$_2$ & Cases	**0.22**	**0.00**	0.13	0.08	0.13	0.06
October		PM$_{2.5}$ & Cases	**0.32**	**0.00**	**0.28**	**0.00**	**0.17**	**0.02**
		PM$_{10}$ & Cases	**0.33**	**0.00**	**0.34**	**0.00**	**0.18**	**0.01**
		NO$_2$ & Cases	**0.32**	**0.00**	**0.20**	**0.00**	**0.15**	**0.03**
August		PM$_{2.5}$ & Death	**0.19**	**0.01**	0.14	0.05	0.11	0.11
		PM$_{10}$ & Death	**0.31**	**0.00**	**0.27**	**0.00**	0.14	0.05
		NO$_2$ & Death	0.11	0.13	0.00	0.95	0.08	0.29
September		PM$_{2.5}$ & Death	**0.22**	**0.00**	**0.18**	**0.01**	**0.19**	**0.01**
		PM$_{10}$ & Death	**0.30**	**0.00**	**0.24**	**0.00**	**0.21**	**0.00**
		NO$_2$ & Death	**0.21**	**0.00**	0.11	0.11	**0.17**	**0.02**
October		PM$_{2.5}$ & Death	**0.28**	**0.00**	**0.24**	**0.00**	**0.15**	**0.03**
		PM$_{10}$ & Death	**0.28**	**0.00**	**0.30**	**0.00**	**0.16**	**0.02**
		NO$_2$ & Death	**0.27**	**0.00**	**0.19**	**0.01**	**0.16**	**0.02**

Values in bold are different from 0 with a significance level alpha = 0.05.

$$y = \sum_{j=1}^{k} f_j + \varepsilon_i \qquad (4)$$

where f_j is the smoothing function introduced in MGWR model, which applied to the jth independent variable and allowed to explore the association at distinct spatial scale/bandwidth.

2.3. Experimental design

Different approaches have been adopted in each segment of the analysis, which collectively demonstrates how forest fire emission can cause severe real-time and lagged impact on the atmosphere and public health. The entire analysis was performed through many successive steps: *first*, the fire affected States, i.e. California, Oregon, Washington, and Colorado, were demarcated based on the number of active fire events statistics and National Fire Emergency Report. These States have been grouped together and named as fire States (short name used as FireStates). The remaining States assumed to have fewer fire effects have been marked as ExFireStates (Excluding fire States). Accordingly, the air pollution assessment was performed for the (a) fire States (FireSates), (b) ExFireStates, and (c) all States (considered both FireStates and ExFireStates), from August 1 to October 30 in both reference year (2019) and fire year (2020). 2019 was chosen as a reference year as this year has comparably lower active fire events than the preceding years. Moreover, OpenAQ air pollution data is available from 2018; this could be another reason for choosing 2019 as a reference year and 2020 as a fire year. 2018 has not been considered in the analysis as there had been high fire events recorded across the Western States of the US, especially in California and surrounding regions (Enders et al., 2021). Since the first forest fire incident occurred sometime in the last week of July and the first week of August, August 1 has been considered the starting date for the analysis. *Second:* the active fire events and their geo-coded information were extracted from Soumi-NPP and NOAA-20 fire products from August 1 to October 30. Other auxiliary information such as FRP, brightness temperature, etc., has also been retrieved from the source data. Instead of taking the weekly period, daily active fire events data was utilized for generating FRP hotspots over the space using the kernel density method. *Third:* sensor location information for PM$_{2.5}$, PM$_{10}$, and NO$_2$ was retrieved from the OpenAQ data platform. Stations with no data (or have irregular data such as missing values or very high/low observation) were discarded from the analysis. Using the approach stated above, a total number of 274, 70 and 61 ground air pollution monitoring stations have been identified for PM$_{2.5}$, PM$_{10}$, and NO$_2$. For few monitoring stations, data was found irregular or not available for either year. These stations have also been removed from the final evaluation. The default unit (ppm) of NO$_2$ was converted to μg/m^3 unit to make it comparable with other pollutants. *Fourth:* The mapping of PM$_{2.5}$, PM$_{10}$, and NO$_2$ was done in two different ways. In the first step, the state-wise average PM$_{2.5}$, PM$_{10}$, and NO$_2$ concentration were measured using the spatial join function in ArcGIS Pro software. The State-wise average concentration of PM$_{2.5}$, PM$_{10}$, and NO$_2$ in the reference year (2019) was provided in supplementary tables. Before putting the pollution estimates into the analysis for spatial mapping and subsequent interpretation, data was checked thoroughly for eliminating outliers and irregular measurements. In the second step, the Inverse Distance Weighted (IDW) kriging was performed using the station's pollution measurements and accordingly, a continuous raster surface was prepared for both fire year and reference year. *Fifth:* The daily concentration of PM$_{2.5}$, PM$_{10}$, and NO$_2$ in the FireStates and ExFireStates from August 1 to October 30 was also incorporated in the assessment to examine the impact of forest fire on air quality of the regions and to statistically assess changes in air pollution concentration during the fire period. The distribution and ranges of the air pollution concentration were measured using minimum, first quartile, median, third quartile, and maximum distributions of parameters. Linear trend analysis was also performed for assessing the changes in PM$_{2.5}$, PM$_{10}$, and NO$_2$ concentration during the study period. Linear trend fit and statistical significance of the change estimates were also measured at different probability levels for the defined period for both 2019 and 2020. Daily PM$_{2.5}$, PM$_{10}$, and NO$_2$ values have been used for the linear trend assessment. Daily COVID-19 cases and deaths counts have also been incorporated into the change assessment analysis to examine the association between air pollution concentration and COVID incidents in the fire-prone States of the US. All the statistical analysis was performed in R statistical software. Multiscale Geographically Weighted Regression (MGWR) was done using the MGWR Python package and MGWRv4 software.

3. Results

3.1. Forest fire emission and its impact on air pollution

The distribution of major forest fire events in the West Coast of the US are provided in Fig. 1. Major fire events were predominantly occurred in California, Oregon, and Washington States. A spatially
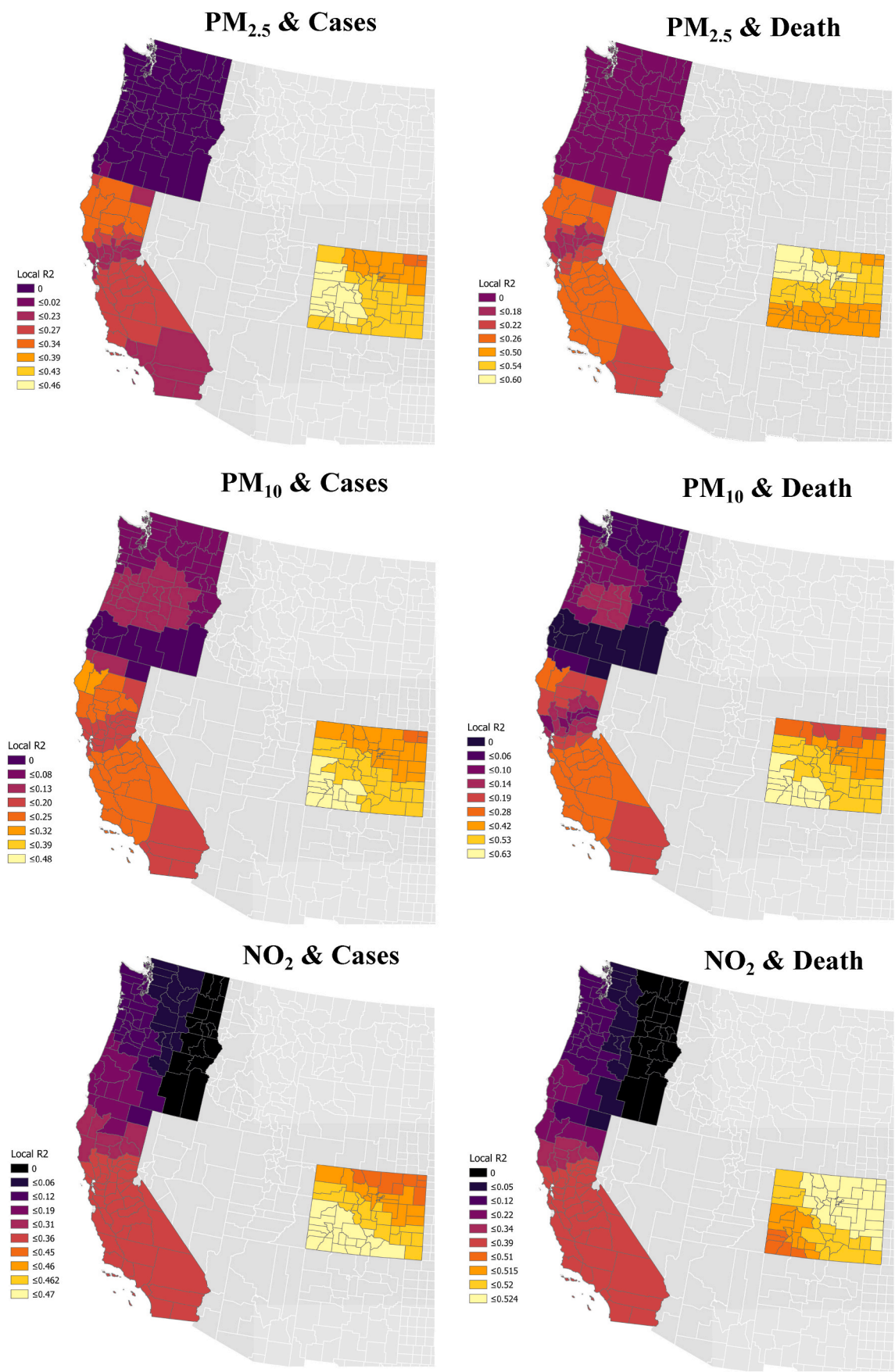
Fig. 11. Spatial coefficient of determination values (R^2) exhibiting the spatial association between air pollution estimates and COVID incidents at local scale.

Fig. 12. Spatial coefficient of determination values (R^2) exhibiting the spatial association between air pollution estimates and COVI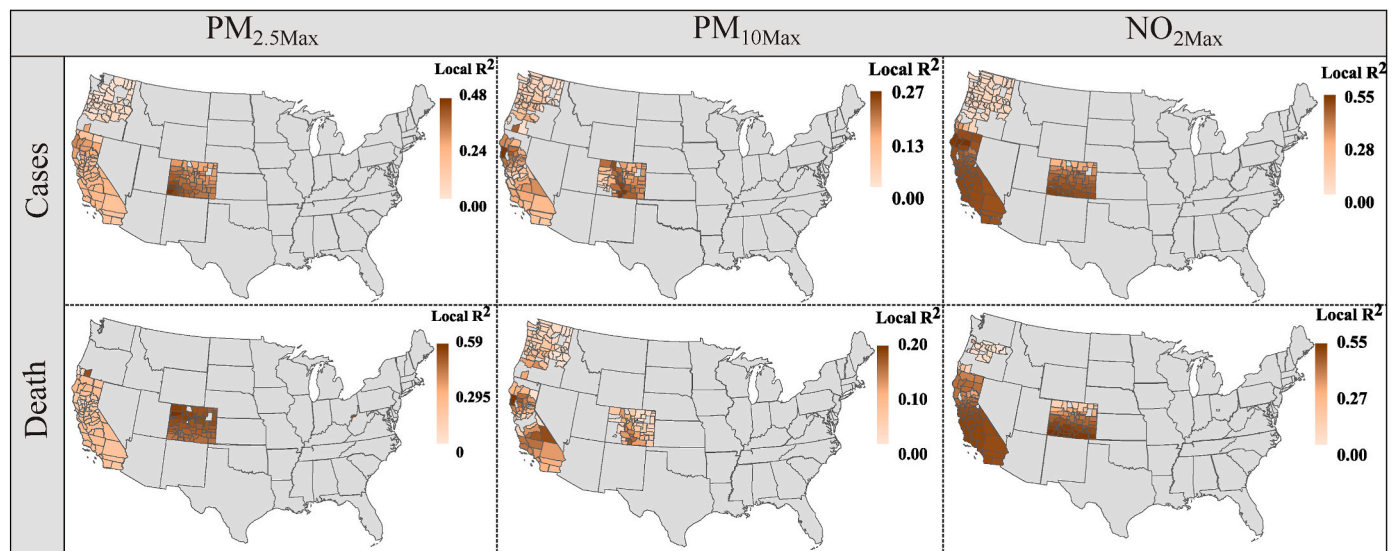D incidents at local scale. $PM_{2.5Max}$, PM_{10Max}, NO_{2Max} refers to the maximum average estimates of $PM_{2.5}$, PM_{10}, and NO_2 measured during the study period.

Table 3
Spatial regression estimates derived from MGWR model. A total of 18 models were developed for both cases and death factors.

Month	Models	R^2	Adj. R^2	AIC	AICc	BIC	Adj.t-value (95%)
Cases							
August	$PM_{2.5}$&Cases	0.348	0.308	497.192	499.025	537.981	2.067
	PM_{10}&Cases	0.336	0.294	501.132	502.987	542.174	2.125
	NO_2&Cases	0.428	0.404	464.078	464.968	492.349	2.527
September	$PM_{2.5}$&Cases	0.33	0.288	502.922	504.816	544.398	2.157
	PM_{10}&Cases	0.326	0.284	503.741	505.586	544.671	2.087
	NO_2&Cases	0.428	0.404	464.168	465.07	492.617	2.544
October	$PM_{2.5}$&Cases	0.257	0.211	522.761	524.573	563.323	2.03
	PM_{10}&Cases	0.254	0.208	523.633	525.476	564.54	2.088
	NO_2&Cases	0.322	0.297	496.051	496.808	522.051	2.563
Death							
August	$PM_{2.5}$&Death	0.314	0.272	506.949	508.722	547.059	2.006
	PM_{10}&Death	0.306	0.262	509.7	511.555	550.739	2.126
	NO_2&Death	0.401	0.377	472.848	473.718	500.788	2.528
September	$PM_{2.5}$&Death	0.255	0.228	514.256	515.011	540.227	2.224
	PM_{10}&Death	0.248	0.222	515.462	516.156	540.316	2.103
	NO_2&Death	0.461	0.438	452.571	453.469	480.958	2.544
October	$PM_{2.5}$&Death	0.291	0.247	513.541	515.354	554.117	2.033
	PM_{10}&Death	0.287	0.243	514.742	516.585	555.649	2.088
	NO_2&Death	0.428	0.407	462.975	463.78	489.815	2.561

scattered fire events are also evident in Colorado, Arizona, Utah, and Montana States (Fig. 1). The spatial-temporal changes and variation of different air pollutants, i.e., $PM_{2.5}$, PM_{10}, and NO_2, were measured using in-situ monitored air pollution data collected from OpenAQ controlled stations. Fig S1 shows the spatial location and distribution of $PM_{2.5}$, PM_{10}, and NO_2 ground monitoring stations. Using the spatially distributed monitoring data, the raster map of different air pollutants have been prepared (Fig. 2, Fig. 3, Fig. 4, Fig. S2; Fig. S3). A drastic change and upsurges of air pollution concentration ($\mu g/m^3$) are evident in the Western part of the US that mainly caused by the 2020 West Coast forest fire events. The maximum $PM_{2.5}$ ($\mu g/m^3$) concentration is recorded as ~80, ~250, and ~160 in August, September, and October in 2020, while the same was recorded much lower in concentration, i.e., ~25, ~65, ~45 during the same period in 2019 (Fig. 2). A similar changing pattern is observed for PM_{10} and NO_2 concentration during the study period (Figs. 3 and 4). PM_{10} concentration ($\mu g/m^3$) is reached up to ~260 in 2020 in the Western states of the US. In contrast, the concentration of PM_{10} is recorded as much lower in 2019. In addition to the raster based analysis, the State averaged pollution concentration ($\mu g/m^3$) is also measured for both 2019 and 2020 (Fig. S2). To save space,

only 2020's map is provided in this paper. The state-averaged concertation values of different air pollutants are found comparably higher in the Western states than the rest of the states of the US. Moreover, the state-averaged change statistics also suggesting a noticeable percentage increases in $PM_{2.5}$, PM_{10}, and NO_2 concentration during the study period. Among the pollutants, the changes are measured highest for $PM_{2.5}$, followed by PM_{10}, and NO_2, respectively (Fig. S3 **and** Fig. S4). Additionally, a high percentage of increases are observed in the fire-affected States, i.e., California, Colorado, Washington, Nebraska, etc. (Fig. S4). While the other States have shown a negligible to negative (air quality index increases in 2020 due to full/partial COVID lockdown in most of the States) changes in air pollution concentration ($\mu g/m^3$) during August 1 to October 31 period in non-fire (2019) and fire year (2020).

The temporal changes in air pollution concentration during the August 1 to October 30 period is evaluated for both 2019 and 2020 and presented in Fig. 5, Fig. 6, Fig. 7, Fig. 8, Table 1, Table S1, Table S2, Table S3, Table S4, Table S5, and Table S6. Fig. 5 and Table. S1 shows the monthly averaged concentration ($\mu g/m^3$) of $PM_{2.5}$, PM_{10}, and NO_2 in August, September, and October months. Only fire states (California,

Table 4
Spatial regression estimates derived from the MGWR model showing local association between the average concentration of pollutants during August to October 2020 and COVID cases and death.

Models	R^2	Adj. R^2	AIC	AICc	BIC	Adj.t-value (95%)
Cases						
$PM_{2.5}$Max&Cases	0.315	0.272	507.041	508.87	547.793	2.039
$PM_{2.5}$Mean&Cases	0.32	0.278	505.489	507.304	546.077	2.044
PM_{10}Max&Cases	0.318	0.275	506.058	507.87	546.624	2.025
PM_{10}Mean&Cases	0.313	0.27	507.599	509.449	548.59	2.094
NO_2Max&Cases	0.542	0.525	418.836	419.581	444.619	2.489
NO_2Mean&Cases	0.409	0.385	470.152	471.012	497.921	2.543
Death						
$PM_{2.5}$Max&Death	0.315	0.272	506.897	508.726	547.649	2.039
$PM_{2.5}$Mean&Death	0.318	0.276	506.007	507.821	546.595	2.044
PM_{10}Max&Death	0.319	0.277	505.607	507.42	546.173	2.026
PM_{10}Mean&Death	0.314	0.271	507.477	509.327	548.468	2.094
NO_2Max&Death	0.556	0.54	412.673	413.4	438.141	2.49
NO_2Mean&Death	0.443	0.421	458.315	459.175	486.084	2.543
Models	R^2	Adj. R^2	AIC	AICc	BIC	Adj.t-value (95%)
Cases						
$PM_{2.5}$Max&Cases	0.315	0.272	507.041	508.87	547.793	2.039
$PM_{2.5}$Mean&Cases	0.32	0.278	505.489	507.304	546.077	2.044
PM_{10}Max&Cases	0.318	0.275	506.058	507.87	546.624	2.025
PM_{10}Mean&Cases	0.313	0.27	507.599	509.449	548.59	2.094
NO_2Max&Cases	0.542	0.525	418.836	419.581	444.619	2.489
NO_2Mean&Cases	0.409	0.385	470.152	471.012	497.921	2.543
Death						
$PM_{2.5}$Max&Death	0.315	0.272	506.897	508.726	547.649	2.039
$PM_{2.5}$Mean&Death	0.318	0.276	506.007	507.821	546.595	2.044
PM_{10}Max&Death	0.319	0.277	505.607	507.42	546.173	2.026
PM_{10}Mean&Death	0.314	0.271	507.477	509.327	548.468	2.094
NO_2Max&Death	0.556	0.54	412.673	413.4	438.141	2.49
NO_2Mean&Death	0.443	0.421	458.315	459.175	486.084	2.543

Oregon, Washington, and Colorado) were considered for calculating the monthly statistical distribution of air pollutants in 2019 and 2020. Monthly averaged $PM_{2.5}$ concentration ($\mu g/m^3$) in 2019 was measured as 7.41, 6.79, 5.49, and 5.96 for California, Colorado, Oregon, and Washington, while the same was measured as 20.95, 14.50, 6.46, and 5.09 in 2020, respectively (Table S1 and Fig. 5). For PM_{10}, the monthly averaged values ($\mu g/m^3$) were increased in the fire affected states (Table S1). However, for NO_2, a decreasing monthly averaged concentration ($\mu g/m^3$) was observed during the study period (Fig. 6 and Table S1). Changes in air pollution concentration due to forest fire are also examined and presented in Figs. 6 and 7, Table 1, and Table S2. During the entire study period (August 1 to October 30), changes in $PM_{2.5}$ was measured highest for Oregon, followed by Washington, California, and Colorado, respectively (Table S2). For PM_{10}, the changes (positive) were highest in Washington, while the same measured comparably low in California and Colorado states (Table S2). Among the three air pollutants, changes in percentage concentration were found lowest for NO_2, as many States have shown the declining status of NO_2 concentration in 2020 (Table S2). This happened due to the partial/fully lockdown imposed in many states due to the outbreak of COVID in 2020. In addition to this, the State-wise monthly averaged concentration of $PM_{2.5}$, PM_{10}, and NO_2 is also measured and presented in Fig. 6, Table S3, Table S4, Table S5. These tables and figures collectively suggest that $PM_{2.5}$, PM_{10}, and NO_2 concentrations were increased in 2020, mainly due to the record-breaking forest fires in the West Coast regions of the contiguous US in 2020. A linear trend curve is also fitted for three air pollutants for both 2019 and 2020 to examine the changes in daily $PM_{2.5}$, PM_{10}, and NO_2 concentration during the study period. The daily averaged linear fit surface measured for both 2019 and 2020 was found significantly high in 2020 than that of 2019. Additionally, the peak $PM_{2.5}$ and PM_{10} concentration ($\mu g/m^3$) have reached up to ~100 (for $PM_{2.5}$) and 200 (for PM_{10}), whereas the daily concentration of the pollutants was measured much lower in 2019, reached maximum up to 25 (for $PM_{2.5}$) and 150 (for PM_{10}), respectively (Fig. 7). Statistical non-

parametric test has been done to examine the mean difference in $PM_{2.5}$, PM_{10}, and NO_2 concentration between fire (2020) and reference (2019) year and presented in Table 1. The mean differences of all three air pollutants, i.e., $PM_{2.5}$ (reported as model 1, 4, 7), PM_{10} (model 2, 5, 8) and NO_2 (model 3, 6, 9) between fire and the non-fire year was found statistically significant at significance level $P < 0.05$ (Table 1). In continuation to the comparison analysis between the air pollution concentration in fire and non-fire years, the monthly averaged air quality index (AQI) is also computed using EPA's defined AQI threshold values. AQI has been found to deteriorate in 2020 in California, Colorado, Idaho, Oregon, Washington, etc. (Table S6). These States have been affected badly by the 2020 forest fire, and a considerable amount of forest area (acres) has been lost that resulted in adding a substantial amount of fine and coarse particulate matter into the atmosphere. The added concentration of $PM_{2.5}$, PM_{10}, and NO_2 that has been observed in this study could be entirely due to forest fire emission, as most the States and large cities in the contiguous US undergone strict lockdown in 2020 to prevent the spread of COVID-19, which means the contribution of anthropogenic emission that comes from traffic and industry is halted and therefore the same has negligible contribution to the increases of air pollution concentration in 2020.

3.2. Forest fire led emission and its association with COVID counts

Fig. 8 shows how COVID new cases/death counts and the concentration of $PM_{2.5}$, PM_{10}, and NO_2 have changed on a daily scale during the study period. For California and Colorado, a synergistic association between the daily $PM_{2.5}$, PM_{10}, and NO_2 concentration and COVID numbers are observed. For the remaining two States, i.e., Oregon and Washington, no such close association between the fire emission and COVID counts have observed (Fig. 8). To further extend the correlation analysis, a correlation matrix has been drawn consisting of month-wise distribution of air pollution estimates and COVID counts in the fire States (Fig. 9, Fig. 10). Fig. 9 was illustrated using the COVID and air

Table 5

Summary table showing the reviewed studies that examined the association between air pollution ($PM_{2.5}$, PM_{10} and NO_2) and COVID-19 cases/deaths.

Pollutants	Author	Study area	Time period	Method used	Main findings
$PM_{2.5}$	Zhu et al. (2020)	120 cities in China	January 23 to February 29, 2020	Generalized Additive Model (GAM)	10 µg/m³ increase in $PM_{2.5}$ was associated with a 2.24% increase in daily COVID-19 confirmed cases
	Fattorini and Regoli (2020)	71 Italian province	February 24 to April 27, 2020	Pearson correlation and regression analysis	$R^2 = 0.340$ (p < 0.01) with total confirmed cases
	Yao et al. (2020)	Wuhan	January 19 to March 15, 2020	Time series analysis	CFR of COVID-19 increased by 0.86% (0.50%–1.22%) each 10 µg/m³ increase in $PM_{2.5}$
	Li et al. (2020)	Wuhan and XiaoGan	January 26 to February 29, 2020	Simple linear regression	$R^2 = 0.174$ (Wuhan), $R^2 = 0.23$ (XiaoGan) with daily confirmed cases
	Yao et al. (2020)	49 cities of China	Up to March 22, 2020	Multiple linear regression	10 µg/m³ increase in $PM_{2.5}$ was associated with a 0.24% (0.01%–0.48%) increase in daily COVID-19 fatality rate
	Zoran et al. (2020a)	Milan (Italy)	January 01 to April 30	Pearson coefficient correlation	r = −0.39; r = 0.25; r = −0.53 for total cases, daily confirmed cases, and total deaths
	Frontera et al. (2020)	Italian regions	Up to March 31, 2020	Pearson correlation and regression analysis	$R^2 = 0.64$; p < 0.01 with total confirmed cases and $R^2 = 0.53$; p < 0.05 with deaths
	Wu et al. (2020)	3000 counties in the U.S.A.	Up to April 04, 2020	Zero-inflated negative binomial models	1 µg/m³ long-term exposure increase in $PM_{2.5}$ was associated with a 15% increase in COVID-19 death rate
	Adhikari and Yin (2020)	Queens county, New York, USA	March 01 to April 20, 2020	Negative binomial regression model	Coefficient of estimates - 0.4029 for daily confirmed cases and −0.1151 for total death
	Vasquez-Apestegui et al. (2021)	24 districts of Lima, Perù	Up to June 12, 2020	Multivariate regression model	Crude coefficient = 0.083, p < 0.05 (for total confirmed cases); Crude coefficient = 0.0016, p < 0.01 (for death); Crude coefficient = −0.014, p > 0.05 (for case fatality rate)
	Bashir et al. (2020)	California, USA	March 04 to April 24, 2020	Spearman and Kendall correlation	Kendall r (−0.359); Spearman r (−0.453) (for confirmed cases); Kendall r (−0.339); Spearman r (−0.429) (for death);
	Travaglio et al. (2021)	England	February 1 and April 8, 2020	generalized linear models, negative binomial regression	an increase of 1 m³ in the long-term average of $PM_{2.5}$ was associated with a 12% increase in COVID-19 cases.
	Magazzino et al. (2020)	Paris, Lyon, and Marseille, Paris	March 18 to April 27, 2020	Artificial Neural Networks (ANNs)	found new threshold levels of $PM_{2.5}$ for COVID-19: 17.4 µg/m³ ($PM_{2.5}$) for Paris, 15.6 µg/m³ ($PM_{2.5}$) for Lyon; 14.3 µg/m³ ($PM_{2.5}$) for Marseille. Marseille, an increase in $PM_{2.5}$ concentrations above 14.3 µg/m³ would generate a 79.01% increase in mortality
	Tello-Leal and Macías-Hernández (2021)	Victoria, Mexico	February 16 to June 06, 2020	Pearson correlation analysis	Pearson r = 0.77 (last four weeks of the partial lockdown) and 0.64 (twelve weeks of the partial lockdown) with total COVID-19 confirmed cases.
	Wu et al. (2020)	3089 counties in the United States	Up to June 18, 2020	Negative binomial mixed model	1 µg/m³ in the long-term average $PM_{2.5}$ is associated with a statistically significant 11% (95% CI, 6–17%) increase in the county's COVID-19 mortality rate.
	Pozzer et al. (2020)	Global	2019	Global atmospheric chemistry general circulation model (EMAC)	Globally, $PM_{2.5}$ contributed to 15% (95% CI 7–33%) COVID-19 mortality, 27% (CI 13–46%) in East Asia, 19% (CI 8–41%) in Europe, and 17% (CI 6–39%) in North America.
	Wu et al. (2021)	326 prefectures in mainland China	Up to April 21, 2020	Negative binomial regression, Spearman's rank correlation	1 µg m³ increase of $PM_{2.5}$ can result in 1.95% (95% CI: 0.83–3.08%) rise of COVID-19 morbidity. Spearman's r = 0.35 (for COVID-19 morbidity counts).
	This study	196 County of California, Colorado, Oregon, and Washington, USA	August 01 to October 30, 2020	Spearman correlation, Ordinary Least Square Regression, Multiscale Geographically weighted regression, Negative binomial regression	Spearman's r = 0.26 (for daily confirmed cases) and r = 0.23 (for death)
PM_{10}	Zhu et al. (2020)	120 cities in China	January 23 to February 29, 2020	Generalized Additive Model (GAM)	10 µg/m³ increase in PM_{10} was associated with a 1.76% increase in daily COVID-19 confirmed cases
	Coccia (2021)	55 Italian province capitals	March 17, 2020 to April 7, 2020	Hierarchical multiple regression model	Cities with having more than 100 days of air pollution (exceeds the limits set for PM_{10}) have a very high average number of infected people (about 3350)
	Fattorini and Regoli (2020)	62 Italian province	February 24 to April 27, 2020	Pearson correlation and regression analysis	$R^2 = 0.267$ (p < 0.01) with total confirmed cases
	Yao et al. (2020)	Wuhan	January 19 to March 15, 2020	Time series analysis	Fatality rate of COVID-19 increased by 0.83% (0.49%–1.17%) for each 10 µg/m³ in PM_{10}
	Li et al. (2020)	Wuhan and XiaoGan	January 26 to February 29, 2020	Simple linear regression	$R^2 = 0.105$ (Wuhan), $R^2 = 0.158$ (XiaoGan) with daily confirmed cases
	Yao et al. (2020)	49 cities of China	Up to March 22, 2020	Multiple linear regression	

Table 5 (*continued*)

Pollutants	Author	Study area	Time period	Method used	Main findings
					$10\ \mu g/m^3$ increase in PM_{10} was associated with a 0.26% (0.00%–0.51%) increase in daily COVID-19 fatality rate
	Zoran et al. (2020b)	Milan (Italy)	January 01 to April 30	Pearson coefficient correlation	r = −0.30; r = 0.35; r = −0.49 for total cases, daily confirmed cases, and total deaths
	Bashir et al. (2020)	California, USA	March 04 to April 24, 2020	Spearman and Kendall correlation	Kendall r (−0.287); Spearman r (−0.375) (for confirmed cases); Kendall r (−0.267); Spearman r (−0.350) (for death);
	Magazzino et al. (2020)	Paris, Lyon, and Marseille, Paris	March 18 to April 27, 2020	Artificial Neural Networks (ANNs)	found new threshold levels of PM_{10} for COVID-19: $29.6\ \mu g/m^3$ (PM_{10}) for Paris, $20.6\ \mu g/m^3$ (PM_{10}) for Lyon; $22.04\ \mu g/m^3$ (PM_{10}) for Marseille. In the city of Paris, an increase in PM_{10} concentration beyond the $29.6\ \mu g/m^3$ threshold could generate a 63.2% increase in mortality (in a COVID-19 pandemic). For Lyon, any value above $20.6\ \mu g/m^3$ in PM_{10} would generate an increase in deaths of 56.12%.
	Tello-Leal and Macías-Hernández (2021)	Victoria, Mexico	February 16 to June 06, 2020	Pearson correlation analysis	Pearson r = 0.79 (last four weeks of the partial lockdown) and 0.69 (twelve weeks of the partial lockdown) with total COVID-19 confirmed cases.
	Marquès et al. (2021)	Tarragona Province (Catalonia, Spain)	March 8, 2020, and May 10, 2020	Pearson correlation analysis	$R^2 = 0.11$ (Chronic exposure of PM_{10} (2014–2019) and $R^2 = 0.01$ (Outbreak exposure of PM_{10} (2020) with confirmed cases per 1000 persons
	Wu et al. (2021)	326 prefectures in mainland China	Up to April 21, 2020	Negative binomial regression, Spearman's rank correlation	$1\ \mu g\ m^3$ increase of PM_{10} can result in 0.55% (95% CI: −0.05–1.17%), rise of COVID-19 morbidity. Spearman's r = 0.15 (for COVID-19 morbidity counts).
	This study	196 County of California, Colorado, Oregon, and Washington, USA	August 01 to October 30, 2020	Spearman correlation, Ordinary Least Square Regression, Multiscale Geographically weighted regression, Negative binomial regression	Spearman's r = 0.32 (for daily confirmed cases) and r = 0.30 (for death)
NO_2	Zhu et al. (2020)	120 cities in China	January 23 to February 29, 2020	Generalized Additive Model (GAM)	$10\ \mu g/m^3$ increase in NO_2 was associated with a 6.94% increase in daily COVID-19 confirmed cases
	Fattorini and Regoli (2020)	62 Italian province	February 24 to April 27, 2020	Pearson correlation and regression analysis	$R^2 = 0.247$ (p < 0.01) with total confirmed cases
	Li et al. (2020)	Wuhan and XiaoGan	January 26 to February 29, 2020	Simple linear regression	$R^2 = 0.329$ (Wuhan), $R^2 = 0.158$ (XiaoGan) with daily confirmed cases
	Ogen (2020)	66 administrative regions in Italy, Spain, France, Germany	Up to the end of February 2020	Descriptive analysis	83% of COVID-19 fatality in the study regions are associated with $NO_2 > 100\ \mu mol/m^2$ range
	Zoran et al. (2020b)	Milan (Italy)	January 01 to April 30	Pearson coefficient correlation	r = −0.55; r = −0.35; r = −0.58 for total cases, daily confirmed cases, and total deaths
	Bashir et al. (2020)	California, USA	March 04 to April 24, 2020	Spearman and Kendall correlation	Kendall r (−0.514); Spearman r (−0.736) (for confirmed cases); Kendall r (−0.485); Spearman r (−0.731) (for death);
	Huang and Brown (2021)	401 counties of Germany	Up to 13th, September 2020	Poisson log-linear model	$1\ \mu g\ m^3$ increase in long-term exposure to NO_2 increasing the COVID-19 incidence rate by 5.58%
	Marquès et al. (2021)	Tarragona Province (Catalonia, Spain)	March 8, 2020, and May 10, 2020	Pearson correlation analysis	$R^2 = 0.55$ (Chronic exposure of NO_2 (2014–2019) and $R^2 = 0.59$ (Outbreak exposure of NO^2 (2020) with confirmed cases per 1000 persons
	Wu et al. (2021)	326 prefectures in mainland China	Up to April 21, 2020	Negative binomial regression, Spearman's rank correlation	$1\ \mu g\ m^3$ increase of NO_2 can result in 4.63% (95% CI: 3.07–6.22%) rise of COVID-19 morbidity. Spearman's r = 0.37 (for COVID-19 morbidity counts).
	This study	196 County of California, Colorado, Oregon, and Washington, USA	August 01 to October 30, 2020	Spearman correlation, Ordinary Least Square Regression, Multiscale Geographically weighted regression, Negative binomial regression	Spearman's r = 0.21 (for daily confirmed cases) and r = 0.20 (for death)

pollution values individually for each of the four fire States, and Fig. 10 was plotted based on the averaged values of COVID counts and $PM_{2.5}$, PM_{10}, and NO_2 concentration of the four fire States. COVID cases and death were statistically significantly correlated with $PM_{2.5}$ October, PM_{10} October, NO_2 September and $NO2$ October estimates (Fig. 9). However, considering the average COVID-19 numbers and air pollution values of the four fire States, a moderate association between the COVID counts and air pollution was found for all three months considered in this study (Fig. 10, Table 2).

The outcomes of the spatial regression analysis between the averaged (average of three months, i.e., August, September, October) air pollution values and COVID-19 counts are presented in Fig. 11 and Fig. 12. For all the test case experiments between COVID counts and air pollution estimates, comparably high spatial R^2 values are measured for the State of Colorado and California counties. In contrast, lower spatial R^2 values are measured for the counties in Washington and Oregon (Fig. 11 **and** Table 3). This implies a spatially localized association between the explanatory (wildfire emission led air pollution) and response variables

(COVID case and deaths) which may not be explained through a global stationary regression model. A similar pattern of association was found between the county averaged maximum PM$_{2.5}$, PM$_{10}$, and NO$_2$ concentrations and COVID-19 counts (Fig. 12 and Table 4). For the month-wise analysis, a total of 18 spatial models were developed that covered both COVID cases and death and accompanied with relevant model diagnostics tests, including AIC, BIC, adjusted *t*-test, to assess the statistical significance of the models at different probability level and uncertainty estimates that are associated with different model parametrization (Table 3). To capture the overall local association between the explanatory and response variables for the entire study period (August 1 to October 30), a total of 12 spatial regression models were developed by considering the averaged values of the COVID-19 and air pollution estimates (both averaged and maximum values were considered) of the studied fire States (Table 4). Among the models, the highest local R^2 are measured for NO$_2$max (R^2 = 0.542 for cases and R^2 = 0.556 for death) and NO$_2$mean (R^2 = 0.409 for cases and R^2 = 0.443 for death) (Table 4). In addition to the spatial regression, the negative binomial regression is also performed to examine the effect of dispersion into the modelling outcomes (Table S7 for COVID-19 case and Table S8 for COVID-19 death). A total of two NB models were performed to examine the association between the explanatory and response variable with adjusted dispersion effects on the model. For both the models, the α or the estimate of dispersion parameter are found greater than 0, which implies the presence of overdispersion in the data. The positive coefficient values suggest that one unit increases of the predictor variable lead to x unit change in the expected outcome of the response variable. Among the model combinations, the positive coefficients values were found between the PM$_{2.5}$max, PM$_{10}$mean, and NO$_2$max with COVID19 cases Table S7, Table S8. These suggest that one-unit changes in PM$_{2.5}$max, PM$_{10}$mean, and NO$_2$max would increase the COVID-19 cases by 0.014, 0.078, and 0.251 units, respectively. While for the death factor, the coefficient values are measured as 0.085 and 0.260 for PM$_{10}$mean and NO$_2$max (Table S7; Table S11).

4. Discussion

The drastic increases of air pollutants in the mid to late 2020 in the West Coast States of the US indicates that the fires in 2020 not only caused severe impact on wildlife and structural damages of properties, but also added high amounts of gaseous and particulate pollutants including smoke and ash into the atmosphere, raising health emergency amidst the COVID-19 pandemic period. Although the clear connection between health effects and forest fire smoke has not been fully explored, there are substantial evidence that supports the strong association between fire emitted smoke and ash concentration and severe health outcomes. Research has also observed that such effects have often exhibited delayed or lagged consequences, especially for cardiovascular and respiratory cause-specific diseases, and do not usually disappear when air gets clear (Landguth et al., 2020). Due to forest fire and the associated emission of particulate matter, a positive trend in PM$_{2.5}$ and PM$_{10}$ concentration was observed in the North-western and Western United States (the most fire-prone region in the US), compared to the other areas of the country for which a negative trend in PM$_{2.5}$ was recorded during the study period. This positive trend in PM$_{2.5}$ concentration was mainly associated with forest fire, black carbon emission and emission of smoke in the West Coast region. The forest fire smoke emission above the boundary layer is often elevated into the free troposphere through convective lofting where the highspeed winds help travel the smoke to a long distance. The subsidence of this smoke layer occurs at the zone of high surface pressure, which can contribute to the enhancement of surface concentration of fine particulate matter (Miller et al., 2011).

There are many factors responsible for recurring forest fire events in the US's West Coast region. The current year has witnessed the above-normal heatwave (~54 °C temperature recorded in some places in

California in 2020), which triggered the ideal condition for ignition and eventually led to massive forest fires. On the other hand, the cold breezes from neighbouring states, Colorado, have supplied the winds that helped grow the blazes across the region. In line with the previous studies, the present analyses found a comparatively higher forest fire activity, mostly over the Western regions of the US, followed by a significantly uplifting particulate matter concentration. At the same time, other parts of the country exhibited a substantially lower concentration of atmospheric pollutants due to the strict practice of lockdown. Additionally, despite being located in the Coastal region where local wind breeze often subdues the high pollution concentration, the Western Coastal states of the US exhibited high spikes of particulate matter and NO$_2$ concentrations amidst the COVID-19 lockdown period when the anthropogenic emission is partially or entirely switched-off.

The unprecedented and abrupt increase of fine and coarse particulate matter in 2020 has mainly happened due to the forest fire emission. This added concentration in PM$_{2.5}$ and PM$_{10}$ could pose serious health concerns to the residents living in this region. Forest fire smoke causes 339,000 annual global premature mortality (interquartile range: 260,000–600,000) (Johnston et al., 2012). An earlier study that analyzed 61 epidemiological studies linked with a forest fire and human health across the world and reported that daily air pollution levels recorded during or after forest fire events exceeded US EPA regulations (Liu et al., 2015). In many cases, the average PM$_{10}$ concentration during the forest fire period was found 1.2 to 10 times higher than that of non-fire periods (Liu et al., 2015). Among the diseases primarily attributed to forest fire, the respiratory disease was highly associated with forest fire smoke concentration (Liu et al., 2015). In the US, nearly 10% of the population (30.5 million) stayed in the regions where the contribution of forest fire to annual average ambient PM$_{2.5}$ was high (>1.5 µg/m^3). Nearly 10.3 million people experienced unhealthy air quality for more than 10 consecutive days attributed to forest fire and resulted in emissions (Rappold et al., 2017). People with the existing respiratory illness have found to be more susceptible to forest fire air pollution effects, and the upsurges of the demand for rescue medication have been linked to the average exposure time to forest fire smoke in Southern California, US (Vora et al., 2011). Ischemic Heart Disease (IHD) has also been linked to forest fire emission (particularly PM$_{10}$ emission) as an elevated number of IHD related clinic visits were reported during the forest fire seasons in California (Lee et al., 2009).

The statistically significant association between the fire emitted particulate matter and COVID-19 numbers measured from both spatial and non-spatial regression models indicated the strong impact of forest fire and resulted in emission of air pollutants on human health. Since the West Coast forest fire has begun in the mid to late 2020, this gives us a once-in-a-century opportunity to carefully examines the close connection between the two extreme events, i.e. record-breaking forest fire in 2020 and the associated emission of air pollutants and its effects on COVID-19 casualties. Since several studies have already established the fact that high concentration of air pollutants, especially PM$_{2.5}$, PM$_{10}$, and NO$_2$, can exacerbate the spread and overall casualties of COVID-19 across the scale, it is expected that the added amount of particulate matter and NO$_2$ concentration will have a significant impact on the overall COVID scenarios of the country. A table has been prepared that summarizes previous research findings and shows how different air pollutants have affected COVID spread and overall casualties caused by COVID-19. Among the studies, Wu et al. (2020) analyzed COVID data from 3000 counties in the US and found that the increases in 1 µg/m^3 PM$_{2.5}$ were associated with increased COVID case by about 15% (Table 5). The results of the negative binomial regression of the present study have also indicated a similar association between the predictors and response variables. This study found that both average and maximum concentration of the key air pollutants are highly associated with the COVID cases and deaths in the fire States considered in this study. More detailed analysis with updated COVID-19 data and air pollution measurements will allow us to explore the actual and lagged

impact of the 2020 forest fires on both the atmosphere and COVID casualties.

5. Conclusion

The present research has evaluated the effects of forest fire on air quality and COVID-19 casualties in the West Coast states (California, Colorado, Oregon, and Washington) in the US. In 2020, the West Coast forest fires broke the past forest fire records, and nearly 8 million acres forest areas were burned in California, Colorado, Oregon, and Washington states in the US. To understand the adverse effects of forest fire emissions on air quality, the concentrations of different air pollutants, i. e., $PM_{2.5}$, PM_{10}, and NO_2, were measured using in-situ monitored data for a fixed period (August 1 to October 30) for 2020 (the fire year) and 2019 (the reference year). Additionally, both spatial and non-spatial regression analysis is performed using the county scale COVID-19 and air pollution data to better understand the adverse effects of fire emission on human health. The concentration of particulate matter and NO_2 increased from three to five times during the fire period in 2020. The abundance of dry fuel load and increasing surface and air temperature has portrayed the potential risk of large-scale fire events in the Western region of the US. Due to the unprecedented forest fire and particulate matter, and gaseous emissions, the average level of exposure to hazardous pollutants has been increased significantly. This may cause severe health hazards if the fire smoke persists over an extended period. The high-intensity fire events in West Coast regions have been triggered by many causal factors, including heatwaves and a warming climate, the abundant load of dry fuel and lack of soil moisture, cold breezes from nearby states and the occurrence of hurricanes amid the fire events. The increased level of air pollution caused by the West Coast forest fire in 2020 revealed a statistically significant positive association with the COVID-19 casualties. This suggest that forest fire and resulted in gaseous and particulate matter emission could play a major role if the same occurs together with a pandemic or epidemic situation.

Credit author statement

Srikanta Sannigrahi: Conceptualization, Data curation, Formal analysis, Writing – review & editing. Francesco Pilla: Conceptualization, Supervision, Writing – review & editing. Arabinda Maiti: Conceptualization, Writing – review & editing. Qi Zhang: Conceptualization, Writing – review & editing. Somnath Bar: Conceptualization, Writing – review & editing. Sandeep Bhatt: Writing – review & editing. Ankit kaparwan: Writing – review & editing. Saskia Keesstra: Conceptualization, Writing – review & editing. Artemi Cerda: Conceptualization, Writing – review & editing.

Declaration of competing interest

The authors declare that they have no known competing financial interests or personal relationships that could have appeared to influence the work reported in this paper.

Appendix A. Supplementary data

Supplementary data to this article can be found online at https://doi.org/10.1016/j.envres.2022.112818.

References

Adhikari, A., Yin, J., 2020. Short-term effects of ambient ozone, PM2. 5, and meteorological factors on COVID-19 confirmed cases and deaths in Queens, New York. Int. J. Environ. Res. Publ. Health 17 (11), 4047. https://doi.org/10.3390/ijerph17114047.

Aponte, C., de Groot, W.J., Wotton, B.M., 2016. Forest fires and climate change: causes, consequences and management options. Int. J. Wildland Fire 25 (i–ii).

Aragão, L.E.O.C., Anderson, L.O., Fonseca, M.G., Rosan, T.M., Vedovato, L.B., Wagner, F. H., Silva, C.V.J., Silva Junior, C.H.L., Arai, E., Aguiar, A.P., Barlow, J., Berenguer, E., Deeter, M.N., Domingues, L.G., Gatti, L., Gloor, M., Malhi, Y., Marengo, J.A., Miller, J.B., Phillips, O.L., Saatchi, S., 2018. 21st Century drought-related fires counteract the decline of Amazon deforestation carbon emissions. Nat. Commun. 9, 536. https://doi.org/10.1038/s41467-017-02771-y.

Badarinath, K.V.S., Kumar Kharol, S., Kiran Chand, T.R., Parvathi, Y.G., Anasuya, T., Jyothsna, A.N., 2007. Variations in black carbon aerosol, carbon monoxide and ozone over an urban area of Hyderabad, India, during the forest fire season. Atmos. Res. 85, 18–26. https://doi.org/10.1016/j.atmosres.2006.10.004.

Balch, J.K., Bradley, B.A., Abatzoglou, J.T., Nagy, R.C., Fusco, E.J., Mahood, A.L., 2017. Human-started forest fires expand the fire niche across the United States. Proc. Natl. Acad. Sci. Unit. States Am. 114, 2946. https://doi.org/10.1073/pnas.1617394114. LP – 2951.

Bashir, M.F., Jiang, B., Komal, B., Bashir, M.A., Farooq, T.H., Iqbal, N., Bashir, M., 2020. Correlation between environmental pollution indicators and COVID-19 pandemic: a brief study in Californian context. Environ. Res. 187, 109652. https://doi.org/10.1016/j.envres.2020.109652.

Bowman, D.M.J.S., Johnston, F.H., 2005. Forest fire smoke, fire management, and human health. EcoHealth 2, 76–80. https://doi.org/10.1007/s10393-004-0149-8.

Chang, L.-Y., 2005. Analysis of freeway accident frequencies: negative binomial regression versus artificial neural network. Saf. Sci. 43, 541–557. https://doi.org/10.1016/j.ssci.2005.04.004.

Cheng, L., McDonald, K.M., Angle, R.P., Sandhu, H.S., 1998. Forest fire enhanced photochemical air pollution. A case study. Atmos. Environ. 32, 673–681. https://doi.org/10.1016/S1352-2310(97)00319-1.

Coccia, M., 2021. How do low wind speeds and high levels of air pollution support the spread of COVID-19? Atmos. Pollut. Res. 12 (1), 437–445. https://doi.org/10.1016/j.apr.2020.10.002.

Collins, B.M., Miller, J.D., Knapp, E.E., Sapsis, D.B., 2019. A quantitative comparison of forest fires in central and northern California under early (1911–1924) and contemporary (2002–2015) fire suppression. Int. J. Wildland Fire 28, 138–148.

Copat, C., Cristaldi, A., Fiore, M., Grasso, A., Zuccarello, P., Signorelli, S.S., Conti, G.O., Ferrante, M., 2020. The role of air pollution (PM and NO2) in COVID-19 spread and lethality: a systematic review. Environ. Res. 191, 110129. https://doi.org/10.1016/j.envres.2020.110129.

Delp, W.W., Singer, B.C., 2020. Professional PM 2 . 5 Monitors with Optical Sensors.

Fattorini, D., Regoli, F., 2020. Role of the chronic air pollution levels in the Covid-19 outbreak risk in Italy. Environ. Pollut. 264, 114732. https://doi.org/10.1016/j.envpol.2020.114732.

Flannigan, M.D., Stocks, B.J., Wotton, B.M., 2000. Climate change and forest fires. Sci. Total Environ. 262, 221–229. https://doi.org/10.1016/S0048-9697(00)00524-6.

Fowler, C., 2003. Human health impacts of forest fires in the southern United States: a literature review. J. Ecol. Anthropol. 7, 39–63. https://doi.org/10.5038/2162-4593.7.1.3.

Fromm, M.D., Servranckx, R., 2003. Transport of forest fire smoke above the tropopause by supercell convection. Geophys. Res. Lett. 30 https://doi.org/10.1029/2002GL016820.

Frontera, A., Cianfanelli, L., Vlachos, K., Landoni, G., Cremona, G., 2020. Severe air pollution links to higher mortality in COVID-19 patients: The "double-hit" hypothesis. J. Infect. 81 (2), 255–259. https://doi.org/10.1016/j.jinf.2020.05.031.

Goldammer, J.G., Statheropoulos, M., Andreae, M.O., 2008. Chapter 1 impacts of vegetation fire emissions on the environment, human health, and security: a global perspective. In: Bytnerowicz, A., Arbaugh, M.J., Riebau, A.R., Andersen, C.B.T.-D., E S (Eds.), Wildland Fires and Air Pollution. Elsevier, pp. 3–36. https://doi.org/10.1016/S1474-8177(08)00001-6.

Henderson, S.B., Brauer, M., MacNab, Y.C., Kennedy, S.M., 2011. Three measures of forest fire smoke exposure and their associations with respiratory and cardiovascular health outcomes in a population-based cohort. Environ. Health Perspect. 119 (9), 1266–1271. https://doi.org/10.1289/ehp.1002288.

Henderson, S.B., Burkholder, B., Jackson, P.L., Brauer, M., Ichoku, C., 2008. Use of MODIS products to simplify and evaluate a forest fire plume dispersion model for PM10 exposure assessment. Atmos. Environ. 42, 8524–8532. https://doi.org/10.1016/j.atmosenv.2008.05.008.

Hodzic, A., Madronich, S., Bohn, B., Massie, S., Menut, L., Wiedinmyer, C., 2007. Forest fire particulate matter in Europe during summer 2003: meso-scale modeling of smoke emissions, transport and radiative effects. Atmos. Chem. Phys. 7, 4043–4064. https://doi.org/10.5194/acp-7-4043-2007.

Huang, G., Brown, P.E., 2021. Population-weighted exposure to air pollution and COVID-19 incidence in Germany. Spatial Stat. 41, 100480. https://doi.org/10.1016/j.spasta.2020.100480.

Ikemori, F., Honjyo, K., Yamagami, M., Nakamura, T., 2015. Influence of contemporary carbon originating from the 2003 Siberian forest fire on organic carbon in PM2.5 in Nagoya, Japan. Sci. Total Environ. 530–531, 403–410. https://doi.org/10.1016/j.scitotenv.2015.05.006.

Iriti, M., Piscitelli, P., Missoni, E., Miani, A., 2020. Air Pollution and Health: the Need for a Medical Reading of Environmental Monitoring Data.

Jaffe, D., Hafner, W., Chand, D., Westerling, A., Spracklen, D., 2008. Interannual variations in PM2.5 due to forest fires in the Western United States. Environ. Sci. Technol. 42, 2812–2818. https://doi.org/10.1021/es702755v.

Jeong, C.-H., Hopke, P.K., Kim, E., Lee, D.-W., 2004. The comparison between thermal-optical transmittance elemental carbon and Aethalometer black carbon measured at multiple monitoring sites. Atmos. Environ. 38, 5193–5204. https://doi.org/10.1016/j.atmosenv.2004.02.065.

Johnston, F.H., Henderson, S.B., Chen, Y., Randerson, J.T., Marlier, M., DeFries, R.S., Kinney, P., Bowman, D.M.J.S., Brauer, M., 2012. Estimated global mortality

attributable to smoke from landscape fires. Environ. Health Perspect. 120, 695–701. https://doi.org/10.1289/ehp.1104422.

Johnston, F.H., Purdie, S., Jalaludin, B., Martin, K.L., Henderson, S.B., Morgan, G.G., 2014. Air pollution events from forest fires and emergency department attendances in Sydney, Australia 1996–2007: a case-crossover analysis. Environ. Heal. 13, 105. https://doi.org/10.1186/1476-069X-13-105.

Juneng, L., Latif, M.T., Tangang, F.T., Mansor, H., 2009. Spatio-temporal characteristics of PM10 concentration across Malaysia. Atmos. Environ. 43, 4584–4594. https://doi.org/10.1016/j.atmosenv.2009.06.018.

Kane, J.M., Varner, J.M., Metz, M.R., van Mantgem, P.J., 2017. Characterizing interactions between fire and other disturbances and their impacts on tree mortality in western U.S. Forests. For. Ecol. Manage. 405, 188–199. https://doi.org/10.1016/j.foreco.2017.09.037.

Kilmer, J.T., Rodríguez, R.L., 2017. Ordinary least squares regression is indicated for studies of allometry. J. Evol. Biol. 30, 4–12. https://doi.org/10.1111/jeb.12986.

Konovalov, I.B., Beekmann, M., Kuznetsova, I.N., Yurova, A., Zvyagintsev, A.M., 2011. Atmospheric impacts of the 2010 Russian forest fires: integrating modelling and measurements of an extreme air pollution episode in the Moscow region. Atmos. Chem. Phys. 11, 10031–10056. https://doi.org/10.5194/acp-11-10031-2011.

Landguth, E.L., Holden, Z.A., Graham, J., Stark, B., Mokhtari, E.B., Kaleczyc, E., Anderson, S., Urbanski, S., Jolly, M., Semmens, E.O., Warren, D.A., Swanson, A., Stone, E., Noonan, C., 2020. The delayed effect of forest fire season particulate matter on subsequent influenza season in a mountain west region of the USA. Environ. Int. 139, 105668. https://doi.org/10.1016/j.envint.2020.105668.

Lazaridis, M., Latos, M., Aleksandropoulou, V., Hov, Ø., Papayannis, A., Tørseth, K., 2008. Contribution of forest fire emissions to atmospheric pollution in Greece. Air Qual. Atmos. Heal. 1, 143–158. https://doi.org/10.1007/s11869-008-0020-0.

Lee, T.-S., Falter, K., Meyer, P., Mott, J., Gwynn, C., 2009. Risk factors associated with clinic visits during the 1999 forest fires near the Hoopa Valley Indian Reservation, California, USA. Int. J. Environ. Health Res. 19, 315–327. https://doi.org/10.1080/09603120802712750.

Li, H., Xu, X.L., Dai, D.W., Huang, Z.Y., Ma, Z., Guan, Y.J., 2020. Air pollution and temperature are associated with increased COVID-19 incidence: a time series study. Int. J. Infect. Diseases 97, 278–282. https://doi.org/10.1016/j.ijid.2020.05.076.

Liu, J.C., Pereira, G., Uhl, S.A., Bravo, M.A., Bell, M.L., 2015. A systematic review of the physical health impacts from non-occupational exposure to forest fire smoke. Environ. Res. 136, 120–132. https://doi.org/10.1016/j.envres.2014.10.015.

Lü, A., Tian, H., Liu, M., Liu, J., Melillo, J.M., 2006. Spatial and temporal patterns of carbon emissions from forest fires in China from 1950 to 2000. J. Geophys. Res. Atmos. 111 https://doi.org/10.1029/2005JD006198.

Magazzino, C., Mele, M., Schneider, N., 2020. The relationship between air pollution and COVID-19-related deaths: an application to three French cities. Appl. Energy 279, 115835. https://doi.org/10.1016/j.apenergy.2020.115835.

Maiti, A., Zhang, Q., Sannigrahi, S., Pramanik, S., Chakraborti, S., Cerda, A., Pilla, F., 2021. Exploring spatiotemporal effects of the driving factors on COVID-19 incidences in the contiguous United States. Sustain. Cities Soc. 68, 102784. https://doi.org/10.1016/j.scs.2021.102784.

Marquès, M., Rovira, J., Nadal, M., Domingo, J.L., 2021. Effects of air pollution on the potential transmission and mortality of COVID-19: a preliminary case-study in Tarragona Province (Catalonia, Spain). Environ. Res. 192, 110315. https://doi.org/10.1016/j.envres.2020.110315.

Martins, V., Miranda, A.I., Carvalho, A., Schaap, M., Borrego, C., Sá, E., 2012. Impact of forest fires on particulate matter and ozone levels during the 2003, 2004 and 2005 fire seasons in Portugal. Sci. Total Environ. 414, 53–62. https://doi.org/10.1016/j.scitotenv.2011.10.007.

Mateus, P., Fernandes, P.M., 2014. In: Reboredo, F. (Ed.), Forest Fires in Portugal: Dynamics, Causes and Policies BT - Forest Context and Policies in Portugal: Present and Future Challenges. Springer International Publishing, Cham, pp. 97–115. https://doi.org/10.1007/978-3-319-08455-8_4.

Matz, C.J., Egyed, M., Xi, G., Racine, J., Pavlovic, R., Rittmaster, R., Henderson, S.B., Stieb, D.M., 2020. Health impact analysis of PM2.5 from forest fire smoke in Canada (2013–2015, 2017–2018). Sci. Total Environ. 725, 138506. https://doi.org/10.1016/j.scitotenv.2020.138506.

McEachern, P., Prepas, E.E., Gibson, J.J., Dinsmore, W.P., 2000. Forest fire induced impacts on phosphorus, nitrogen, and chlorophyll a concentrations in boreal subarctic lakes of northern Alberta. Can. J. Fish. Aquat. Sci. 57, 73–81. https://doi.org/10.1139/f00-124.

McLean, K.E., Yao, J., Henderson, S.B., 2015. An evaluation of the British columbia asthma monitoring system (BCAMS) and PM2.5 exposure metrics during the 2014 forest fire season. Int. J. Environ. Res. Publ. Health. https://doi.org/10.3390/ijerph120606710.

Meira Castro, A.C., Nunes, A., Sousa, A., Lourenço, L., 2020. Mapping the causes of forest fires in Portugal by clustering analysis. Geosci. https://doi.org/10.3390/geosciences10020053.

Michel Arbez, Birot, Yves, Carnus, Jean-Michel, 2001. Risk Management and Sustainable Forestry.

Miller, D.J., Sun, K., Zondlo, M.A., Kanter, D., Dubovik, O., Welton, E.J., Winker, D.M., Ginoux, P., 2011. Assessing boreal forest fire smoke aerosol impacts on U.S. air quality: a case study using multiple data sets. J. Geophys. Res. Atmos. 116 https://doi.org/10.1029/2011JD016170.

Mollalo, A., Vahedi, B., Rivera, K.M., 2020. GIS-based spatial modeling of COVID-19 incidence rate in the continental United States. Sci. Total Environ. 728, 138884. https://doi.org/10.1016/j.scitotenv.2020.138884.

Mott, J.A., Meyer, P., Mannino, D., Redd, S.C., Smith, E.M., Gotway-Crawford, C., Chase, E., 2002. Wildland forest fire smoke: health effects and intervention

evaluation, Hoopa, California, 1999. West. J. Med. 176, 157–162. https://doi.org/10.1136/ewjm.176.3.157.

Ogen, Y., 2020. Assessing nitrogen dioxide (NO2) levels as a contributing factor to coronavirus (COVID-19) fatality. Sci. Total Environ. 726, 138605. https://doi.org/10.1016/j.scitotenv.2020.138605.

Oshan, T.M., Li, Z., Kang, W., Wolf, L.J., Stewart Fotheringham, A., 2019. MGWR: a python implementation of multiscale geographically weighted regression for investigating process spatial heterogeneity and scale. ISPRS Int. J. Geo-Inf. 8 https://doi.org/10.3390/ijgi8060269.

Pio, C.A., Legrand, M., Alves, C.A., Oliveira, T., Afonso, J., Caseiro, A., Puxbaum, H., Sanchez-Ochoa, A., Gelencsér, A., 2008. Chemical composition of atmospheric aerosols during the 2003 summer intense forest fire period. Atmos. Environ. 42, 7530–7543. https://doi.org/10.1016/j.atmosenv.2008.05.032.

Pozzer, A., Dominici, F., Haines, A., Witt, C., Münzel, T., Lelieveld, J., 2020. Regional and global contributions of air pollution to risk of death from COVID-19. Cardiovasc. Res. 116 (14), 2247–2253. https://doi.org/10.1093/cvr/cvaa288.

Randerson, J.T., Liu, H., Flanner, M.G., Chambers, S.D., Jin, Y., Hess, P.G., Pfister, G., Mack, M.C., Treseder, K.K., Welp, L.R., Chapin, F.S., Harden, J.W., Goulden, M.L., Lyons, E., Neff, J.C., Schuur, E.A.G., Zender, C.S., 2006. The impact of boreal forest fire on climate warming. Science 314, 1130–1132. https://doi.org/10.1126/science.1132075.

Rappold, A.G., Reyes, J., Pouliot, G., Cascio, W.E., Diaz-Sanchez, D., 2017. Community vulnerability to health impacts of wildland fire smoke exposure. Environ. Sci. Technol. 51, 6674–6682. https://doi.org/10.1021/acs.est.6b06200.

Sannigrahi, S., Pilla, F., Basu, B., Basu, A.S., 2020a. The overall mortality caused by COVID-19 in the European region is highly associated with demographic composition: a spatial regression-based approach. Work. Pap. 1–43.

Sannigrahi, S., Pilla, F., Basu, B., Basu, A.S., Molter, A., 2020b. Examining the association between socio-demographic composition and COVID-19 fatalities in the European region using spatial regression approach. Sustain. Cities Soc. 62, 102418. https://doi.org/10.1016/j.scs.2020.102418.

Sapkota, A., Symons, J.M., Kleissl, J., Wang, L., Parlange, M.B., Ondov, J., Breysse, P.N., Diette, G.B., Eggleston, P.A., Buckley, T.J., 2005. Impact of the 2002 Canadian forest fires on particulate matter air quality in Baltimore city. Environ. Sci. Technol. 39, 24–32. https://doi.org/10.1021/es035311z.

Sayahi, T., Butterfield, A., Kelly, K.E., 2019. Long-term field evaluation of the Plantower PMS low-cost particulate matter sensors. Environ. Pollut. 245, 932–940. https://doi.org/10.1016/j.envpol.2018.11.065.

Sciomer, S., Moscucci, F., Magrì, D., Badagliacca, R., Piccirillo, G., Agostoni, P., 2020. SARS-CoV-2 spread in Northern Italy: what about the pollution role? Environ. Monit. Assess. 192, 2–4. https://doi.org/10.1007/s10661-020-08317-y.

Shen, H., SHEN, G., Chen, Y., Russell, A., Hu, Y., Duan, X., Meng, W., Xu, Y., Yun, X., Lyu, B., Zhao, S., Hakami, A., Tao, S., Smith, K., 2020. Increased air pollution exposure among the Chinese population during the national quarantine in 2020. https://doi.org/10.31223/osf.io/6d9rn.

Sokal, R.R., Rohlf, F.J., Sokal, R.R., 1995. Biometry : the Principles and Practice of Statistics in Biological Research, 3rd ed. W.H. Freeman, New York.

Spichtinger, N., Wenig, M., James, P., Wagner, T., Platt, U., Stohl, A., 2001. Satellite detection of a continental-scale plume of nitrogen oxides from boreal forest fires. Geophys. Res. Lett. 28, 4579–4582. https://doi.org/10.1029/2001GL013484.

Sullivan, A.P., Holden, A.S., Patterson, L.A., McMeeking, G.R., Kreidenweis, S.M., Malm, W.C., Hao, W.M., Wold, C.E., Collett Jr., J.L., 2008. A method for smoke marker measurements and its potential application for determining the contribution of biomass burning from forest fires and prescribed fires to ambient PM2.5 organic carbon. J. Geophys. Res. Atmos. 113 https://doi.org/10.1029/2008JD010216.

Tello-Leal, E., Macías-Hernández, B.A., 2021. Association of environmental and meteorological factors on the spread of COVID-19 in Victoria, Mexico, and air quality during the lockdown. Environ. Res. 196, 110442. https://doi.org/10.1016/j.envres.2020.110442.

Travaglio, M., Yu, Y., Popovic, R., Selley, L., Leal, N.S., Martins, L.M., 2021. Links between air pollution and COVID-19 in England. Environ. Pollut. 268 https://doi.org/10.1016/j.envpol.2020.115859.

Vasquez-Apestegui, B.V., Parras-Garrido, E., Tapia, V., Paz-Aparicio, V.M., Rojas, J.P., Sanchez-Ccoyllo, O.R., Gonzales, G.F., 2021. Association between air pollution in Lima and the high incidence of COVID-19: findings from a post hoc analysis. BMC Publ. Health 21 (1), 1–13. https://doi.org/10.1186/s12889-021-11232-7.

Vora, C., Renvall, M.J., Chao, P., Ferguson, P., Ramsdell, J.W., 2011. 2007 san diego forest fires and asthmatics. J. Asthma 48, 75–78. https://doi.org/10.3109/02770903.2010.535885.

Wang, C., Li, S., Shan, J., 2021. Non-stationary modeling of microlevel road-curve crash frequency with geographically weighted regression 1–17.

Wang, Pengfei, Chen, K., Zhu, S., Wang, Peng, Zhang, H., 2020. Severe air pollution events not avoided by reduced anthropogenic activities during COVID-19 outbreak. Resour. Conserv. Recycl. 158, 104814. https://doi.org/10.1016/j.resconrec.2020.104814.

Watson, G.L., Telesca, D., Reid, C.E., Pfister, G.G., Jerrett, M., 2019. Machine learning models accurately predict ozone exposure during forest fire events. Environ. Pollut. 254, 112792. https://doi.org/10.1016/j.envpol.2019.06.088.

Wu, J., M Winer, A., J Delfino, R., 2006. Exposure assessment of particulate matter air pollution before, during, and after the 2003 Southern California forest fires. Atmos. Environ. 40, 3333–3348. https://doi.org/10.1016/j.atmosenv.2006.01.056.

Wu, X., Nethery, R.C., Sabath, M.B., Braun, D., Dominici, F., 2020. Air pollution and COVID-19 mortality in the United States: strengths and limitations of an ecological regression analysis. Sci. Adv. 6, 1–7. https://doi.org/10.1126/sciadv.abd4049.

Wu, Y., Zhan, Q., Zhao, Q., 2021. Long-term air pollution exposure impact on COVID-19 morbidity in China. Aerosol Air Qual. Res. 21 (1), 200413. https://doi.org/10.4209/aaqr.2020.07.0413.

Yao, Y., Pan, J., Wang, Weidong, Liu, Z., Kan, H., Qiu, Y., Meng, X., Wang, Weibing, 2020. Association of particulate matter pollution and case fatality rate of COVID-19 in 49 Chinese cities. Environ. Res. 741, 109941. https://doi.org/10.1016/j.scitotenv.2020.140396.

Zhu, Y., Xie, J., Huang, F., Cao, L., 2020. Association between short-term exposure to air pollution and COVID-19 infection: evidence from China. Sci. Total Environ. 727, 138704. https://doi.org/10.1016/j.scitotenv.2020.138704.

Zoran, M.A., Savastru, R.S., Savastru, D.M., Tautan, M.N., 2020a. Assessing the relationship between surface levels of PM2.5 and PM10 particulate matter impact on COVID-19 in Milan, Italy. Sci. Total Environ. 738, 139825. https://doi.org/10.1016/j.scitotenv.2020.139825.

Zoran, M.A., Savastru, R.S., Savastru, D.M., Tautan, M.N., 2020b. Assessing the relationship between ground levels of ozone (O3) and nitrogen dioxide (NO2) with coronavirus (COVID-19) in Milan, Italy. Sci. Total Environ. 740, 140005. https://doi.org/10.1016/j.scitotenv.2020.140005.